THE UNIVERSITY of ADELAIDE

Monitoring Groundwater Flow Using Electrokinetics

By Robert Lampe

School of Earth and Environmental Sciences,

Geology & Geophysics, University of Adelaide

Primary Supervisor: Graham Heinson

Secondary Supervisor: Michael Hatch

Contents

Abstract

Very little is known about the groundwater flow paths from the subsurface of the Great Artesian Basin to the surface basins throughout the Australian continent. The Wabma Kadarbu Mound Springs in northern South Australia lie at the south-west margin of the Great Artesian Basin and contain a number of springs that continually discharge groundwater over time.

This work deals with the self potential (SP) method which was used along three intersecting lines in the area to help gain a better understanding of groundwater flow. The SP method responds to the electrokinetic phenomenon of streaming potential which can be applied to hydrogeological investigations to help evaluate the subsurface groundwater flow conditions. Because the SP data do not intrinsically yield a good indication of the depth of the sources generating groundwater flow, numerical models are developed to assess the SP distribution resulting from subsurface fluid flow.

The self-potential associated with groundwater flow in an electrolytic environment is modelled by assuming a primary source as an electric double layer between the flowing groundwater and the porous media created by the flowing SP currents. This primary flow generates the secondary surface charge and double layers on the interfaces between media with different conductivities. The geometry of the sources is obtained from an image reconstruction technique which determines the spatial locations of SP sources. The modelling and image reconstructions help to obtain a better understanding of these flow paths and how they make their way to the surface can give a greater chance of collecting the groundwater to use to good effect.

The results showed evidence for groundwater flow networks in the subsurface of the Wabma Kadarbu springs. The groundwater flow networks for all three lines had similar characteristics

including having individual columns connected at depth and large widths for the columns. This research showed that SP can be used to help better understand groundwater flow patterns in the subsurface.

Key words: self potential, groundwater, mound springs, electrokinetics, Great Artesian Basin

Introduction

The aim of this project was to investigate the interconnection between groundwater in the Great Artesian Basin (GAB) and the surface water in the Lake Eyre Basin (LEB). This was done by monitoring groundwater flow below the surface of the earth using different geophysical techniques. Five techniques were used and these were Spectral Induced Polarisation (SIP), NanoTEM, Magnetotellurics (MT), Electromagnetics (EM), and Self Potential (SP). This particular paper focuses on the self potential survey that was done over the area.

The Great Artesian Basin (Figure 1) is the largest and deepest artesian basin in the world (Torgersen et al. 1992). It covers 22% (or 1.7 million sq.km) of the Australian continent (Mudd et al. 2000) extending across parts of South Australia, Queensland, New South Wales and the Northern Territory (Habermehl, et al. 1986). The amount of water in the GAB is estimated to be 64 900 million mega litres (DERM, 2011). The Lake Eyre Basin is a drainage basin and is one of the largest internally draining systems in the world (National Heritage Trust, 2005). It covers 14% (or 1.14 million sq.km) of the continent and it covers areas of South Australia, New South Wales, Queensland and the Northern Territory. Much of the area overlaps the GAB.

Rising groundwater from the GAB discharges in the form of Mound Springs which are domed shaped structures. The mound springs help to preserve the local fauna and flora in the area due to the discharge of the water. If the steady flow of the water discharging from the mound springs decreases then this will greatly affect the environment in the area and the landscape would become barren and almost lifeless similar to the areas of the Australian outback that do not have a continuous discharge of water.

Little research has been done on the mound springs in terms of the subsurface water flow. The interconnection between the groundwater in the GAB and the surface water in the LEB is unknown. The water could be from shallow sources or deep sources and the movement could be from seepage to the surface or through faults and fractures. The shallow subsurface fluids could be sourced from recharge of the soils through rainfall, although rainfall is low in this area and therefore recharge would also be low (National Heritage Trust, 2005). The deep sourced subsurface fluids are likely to be from aquifers in the GAB, i.e., from water flow going east to west from the western side of the Great Dividing Range mountain chain in the eastern part of Australia (Habermahl et. al. 1996). The network of fluid flow in the subsurface here is controlled by faults and seepage (habermahl et.al. 1996) and with faults water will flow up in narrow pipes and with seepage water flows up over a broad area.

As the areas of interest are all buried under sedimentary cover, geophysics is a potentially useful tool to help obtain information about the geology and fluid pathways of the area. For this study the SP method was used to help determine the nature of fluid pathways in the subsurface. Three intersecting lines of SP were completed over a 1.5km^2 area at Wabma Kadarbu National Park (Figure 2), in the south-western part of both the LEB and the GAB. This area contains a large network of springs consisting of two major springs, called “The Bubbler” and “Blanche Cup” as well as other smaller springs and extinct mounds that were once active springs.

The Great Artesian Basin Geology and Hydrology

The aquifer system in the GAB is a confined multilayer system and consists of quartzose sandstones interbedded with siltstones, mudstones and shales (Torgerson et al. 1992) (Figure 3). This multilayer system of rock units was formed over millions of years from the deposition and then the silicification of rock forming sediments in three depressions in the GAB; the Carpentaria, Eromanga and the Surat basins.

Sedimentation first occurred towards the end of the Triassic period approximately 200 million years ago when uplift at the margins of these smaller basins produced erosion. Alternating layers of clays, silts, sands and gravels occurred due to variation in the landscape over time with streams, rivers, floodplains and lakes forming at different stages (DERM, 2011). The sandy sediments consolidated to form the permeable sandstone (aquifers) and the clayey sediments consolidated to form the impermeable shales and mudstones. This multilayered system of rock units reaches a maximum depth of 3000 m near the central part of the basin (Habermehl, 2001). In the Cretaceous period, high sea levels produced a shallow inland sea throughout central Australia, depositing muddy sediments, which consolidated to form more impermeable layers. Towards the end of the Cretaceous period, approximately 65 million years ago, uplift and erosion exposed the sandstone aquifers at the margins of the basin, particularly the western margin of the present day Great Dividing Range. Since then rainfall has infiltrated into the sandstones to create the enormous groundwater reserve seen today (DERM, 2011). The Cretaceous sedimentary rocks are overlain by Tertiary sedimentary rocks, and again by Quaternary cover, composed of mainly unconsolidated sediments (Habermehl, 2001).

In the Wabma Kadarbu area the rock sequence composing the confined aquifers in the GAB is bounded by Adelaidean sediments at the bottom, and the Winton Formation at the top (Habermehl, 1983). The major aquifers are present in the Cadna-owie formation, Oodnadatta formation and the Algebuckina sandstone. The major confining bed in this region is the Bulldog shale, which confines both the Cadna-owie formation and the Algebuckina sandstone.

Mound Springs in the Great Artesian Basin

Mound Springs are conical shaped structures and are found throughout the GAB but particularly around the perimeter where they are formed by discharging groundwater. They are composed mostly of carbonates and clastic material and salts but sometimes also form as seeps discharging to the surface with little visible surface expression (National Heritage Trust, 2005). These conical shaped structures become quite big over time, in fact often 20m high as observed in the field. They form around the edges of the GAB because faulting and folding in the subsurface in this area accommodates better interconnection for groundwater to flow between the GAB and the surface.

In the LEB there are 8 different supergroups of mound springs which are divided up into two areas. One group is located close to the recharge zones of the GAB in Queensland and the other is situated in the southern and south-western end of the GAB in northern South Australia (National Heritage Trust, 2005). This group includes the Wabma Kadarbu springs (Figure 2) .

The discharge of water flowing up from these springs is different between summer and winter mostly due to evapotranspiration. In the summer months evapotranspiration is higher due to increased heat and the water evaporates a couple of metres below the ground so does not flow towards the surface. Changes to spring discharges are also affected by changes in artesian

pressure or subartesian groundwater levels. This is because spring flow depends on a pressure gradient between the aquifers in the GAB and the atmosphere. Flow from the springs can vary if the atmospheric pressure is increased, or the pressure in the aquifer is lowered (Friends of Mound Springs, 2007).

Wabma Kadarbu Springs

As mentioned earlier the Wabma Kadarbu springs are located in the south-western edge of the LEB and the GAB (Figure 2) and they consist of a number of springs all of different sizes and with different discharge rates. The main springs in the area are The Bubbler Spring, the Blanche Cup Spring (Figure 5) and the extinct Hamilton Hill Spring. The Bubbler has the fastest discharge rate, with most of the discharge flowing towards the south east. The Wabma Kadarbu area is considerably saltier than the other spring systems in the area including the Beresford and Warburton springs, so the ground is very electrically conductive.

The outcrop of the Wabma Kadarbu Springs area is mainly composed of Bulldog Shale which is a medium to dark grey, silty to fine grained mudstone interbedded with thin beds of coarse to very coarse quartz sand and granules. The new springs themselves are composed of limestone and Mesozoic sediments and the extinct Hamilton Hill is composed more of yellow-grey limestone and minor goethite. (Geological Survey of South Australia, 1992).

Self-Potential and Electrokinetic Theory

Electrokinetics or electrokinetic phenomena are a broad range of different effects that occur in heterogeneous fluids or porous bodies that are filled with fluid. They are geophysical phenomena resulting from the differential movement of two phases where the interface is an electrical double

layer. The electrical double layer of charges is a fundamental concept with electrokinetics (Kim et al. 2004).

The electrical double layer is created when two phases of different chemical constitutions are in contact which develops an electric potential difference between the two phases. This potential difference is accompanied by a charge separation with one side of the interface negatively charged and the other side positively charged (Ishido & Mizutani et al. 1981). The electrical double layer is composed of the immobile part of the fluid, with this part divided into 2 separate layers, the Stern and Diffusion Layers. The hydrodynamic slipping or Stern plane separates the immobile fluid from the mobile fluid (Kim et al. 2004). At this plane the potential that is generated is called the zeta-potential. The zeta-potential can be positive or negative depending on the amount of specific adsorption in the Stern Layer between the pore wall and the boundary between the Stern Layer and the Diffusion Layer. When there are more positive than negative ions transported with the fluid, the zeta-potential is negative (Figure 4). The zeta-potential is an electrochemical property of the pore water/mineral interface, and the pore fluid pressure field (Kim et al. 2004).

In general the electrical double layer refers to two parallel layers of charge surrounding the object in the immobile part of the fluid. For the stern layer, which is the layer closest to the mineral surface, the surface charge (either positive or negative) comprises ions directly adsorbed onto the object due to a host of chemical interactions, including the electrostatic charge. The second layer, or the diffusion layer, is composed of ions attracted, not adsorbed, to the surface charge via the Coulomb force, electrically screening the first layer. It is called the diffuse layer because it is made of free ions which move in the fluid due to the electric attraction and thermal motion, and so it is not fully associated with the mineral (Fagerlund & Heinson 2002). The

particular electrokinetic phenomenon that is relevant to the work being done is the streaming potential which is a type of self-potential (also called spontaneous potential).

Self-potentials (SP) are coupled flows and are naturally occurring electric potential differences in the Earth and are caused by charge separation in minerals below the surface, due to the presence of semi-permeable interface preventing the diffusion of ions through the pore space of rocks, or by natural flow of a conducting fluid through the rocks (Lyklema, 1995). Studies have shown that the self-potential method is an accurate method to measure fluid flow [e.g., Schiavone & Quarto 1984; Aizawa et al., 2005; Bedrosian et al., 2007].

The streaming potential is the potential difference at zero current generated by the flow of liquid under a pressure gradient through a capillary. To measure the streaming potential identical electrodes are placed on each side of the capillary, and it is positive if the higher potential is on the high pressure side. The streaming potentials are created by the flow of the counter charge inside the capillaries (Lyklema, 1995).

As well as streaming potentials the other type of self potentials are electrochemical potentials. EC potentials can be generated as a result of several different phenomena, with the most frequent one being the diffusion of ions due to a concentration gradient between two phases. Redox processes occurring in ore bodies and contaminant plumes are another common EC source mechanism. (Jouniaux et al. 2009).

The self-potential method is very simple and is not very time consuming although the method has been scarcely used in past geophysical studies because multiple sources can generate the potential difference that the self-potential method measures (Sill, 1982). These multiple sources

include EC, EK or a mixture of both sources. The EC potential is the sum of the liquid junction or diffusion potential and membrane potential.

Liquid junction or diffusion potentials occur at liquid-liquid boundaries if the neighbouring phases are made up of ions of differing mobilitys and in different concentrations. Mutual diffusion will take place and when the diffusing species are ions of an electrolyte, one of the ions will move ahead of the other ions, creating a potential difference, i.e., a clear boundary is made between a dilute and a concentrated electrolyte with the cations having a higher mobility than the anions and the cations move ahead of the anions (Lyklema 1995). The membrane potential is the difference in voltage between the interior and exterior of a cell. It is generated when two electrolyte solutions of dissimilar concentration make contact with each other due to the difference in the mobility of cations and anions (Fan & Deng, 2002). EC potentials occur in the subsurface due to chemical changes in the soils in the subsurface.

Methodology

In the field three lines were chosen for SP surveying. They were chosen so as to minimise interference and to maximise the number of features intersected. Station spacing was approximately every 25m and locations were marked using a non-differential Global Positioning System (GPS). Data was collected using a voltmeter to an accuracy of 1mV, a long wire (approximately 1600m), three Cu-Cu-Sulphate electrodes or “pots”, sponges, and a bucket containing enough copper sulphate solution to keep the base of the pots wet.

The fixed base configuration (Corwin, 1990) for self-potential mapping was used opposed to the gradient configuration as this was considered advantageous because of the lower level of cumulative error and the greater efficiency and speed of the method. The normal voltage, reverse

voltage, and the contact resistance were measured at each station. The normal voltage was measured with the base pot wire attached to the negative terminal of the voltmeter, and the roving pot connected to the positive terminal by convention (Corry et al., 1983). The reverse voltage was measured by reversing the polarity of the voltmeter leads and was done to check if there were any problems with the circuit. The contact resistance was measured to determine if the circuit was complete and that there was no interference. A brief description of the regolith of the area was also recorded at each station due to the heterogeneity of the area.

The three pots used were a base pot, which for the fixed base configuration stayed at the base location of the line being conducted, a reference pot, which stayed permanently in the bucket of solution, and a roving pot, which was used at each site along the line to measure the SP between itself and the base pot. Intermediate drift correction values were obtained by periodically reading the potential between the roving pot and the reference pot carried in the solution. Here it was assumed that the potential between the base and the reference pot remained constant, so the drift of the roving pot with respect to the base pot could be computed and removed. The first reading on the line was repeated at the end of the day to establish total daily drift. Sponges soaked in Cu-Cu-Sulphate solution were used in situations where there was no unconsolidated soil to place the pots in to do measurements (Corwin, 1990).

The three self-potential lines all crossed over each other, but not at one exact point. They were of different lengths, and each of them went over different springs. Station spacing was halved if there was a big discrepancy between the normal voltage readings between two stations. Line A was read over two days, using a common position for the base pot. There was a consistent drift difference between the base and roving pots for each station between the two days, so this was corrected. Line B was also read over two days, but with two different base locations that were

tied together (Line B was very long). There was also a consistent drift difference between the base and roving pots for each station between the two days, this was corrected, and a base tie in correction was done to account for a change in base pot location between the two days. Line C was conducted over one day, so only the daily base-roving pot drift voltage had to be accounted for.

Data Processing and Results

Data processing involved using drift corrections and base tie-in corrections to obtain the absolute voltages at each of the different stations for all three lines which is the voltage relative to the survey base for each of the three lines. The exact distances between stations for all lines were determined using the co-ordinates of each station and these distances were used in graphs opposed to the distances obtained out in the field due to the random errors associated with determining station spacing using measuring tape for line A and particularly walking pace for Lines B and C. Graphs were made representing absolute voltage against eastings, distance (Figures 6,7,8) or station and these also included elevation and regolith of the area. A moving three-point average was applied to the data to smooth out short wavelength fluctuations to help with the modelling conducted afterwards.

All three lines had sections that showed a large amount of variability across different varieties of regolith including sands, clays and limestone rocks. This variability is interpreted as to most likely being an EC effect from a large abundance of chemical reactions occurring in the near subsurface. All three lines also had characteristic peaks of SP near springs which were assumed to be as a result of groundwater flow.

Line C showed the most obvious profile for groundwater flow with the second half of the line showing large peaks in the SP at two springs and a smaller peak between the two springs (Figure 8) most likely showing a connection between the groundwater flow of the two springs in the subsurface and possibly another spring forming in the future. The first 600 m of the line is extremely variable and this is thought to be because of EC effects associated with changes in the regolith (see appendix) and also the line going directly over The Bubbler tail and runoff area.

The first 600 m of line B (Figure 7) contained a mixture of sands and silts and had quite a steady pattern with no outstanding peaks or troughs except for a large trough at the start of the line with low levels of SP measured at the first three stations. This line contained three springs including the spring with the fastest flow rate in the area, The Bubbler, at 1450 m along the line. The SP response at all three springs was high compared to the other areas along the line most likely due to EK effects, although increased elevation for two of these three springs would generate slightly higher responses than if they were at a similar elevation to the rest of the line. The SP response for the Bubbler was quite wide, reaching almost 300 m, suggesting an extensive groundwater flow pattern in the subsurface. With the area around the Bubbler being very homogeneous in terms of regolith (sandy), this greatly decreases the chances for an EC effect here.

Line A (Figure 6) showed a large amount of variability for the first 400m across a mixture of limestone rocks and sands and an EC effect was thought to have caused this. A peak occurs at 450 m along the line in a more clayey regolith area and is approximately 180m wide. It is situated just east of the Little Bubbler over the springs runoff area which goes in an easterly direction then diverts south. Another peak was also found at 950m along the line in an area consisting of sands and vegetation and was approximately 200m wide. These were most likely due to EK effects generated by groundwater flow under the springs.

Modelling

Interpreting electrokinetic potential data is difficult because it may involve a number of different interdependent parameters. To interpret the data it is fully required to develop a modelling algorithm (Kim et. al, 2004). A few different modelling techniques were used to try and give an indication of the groundwater flow network in the subsurface. One method was from Sheffer and Oldenburg, (2007). Their forward model involved a 3-D finite volume algorithm for calculating the SP distribution resulting from fluid flow from a point injection well in a porous medium. An analytical solution was calculated from the following equation, given by;

$$\emptyset = \frac{LQ(r_s)v_s}{2\pi\sigma K\,|r-r_s|}$$

where $\emptyset$ is the electric potential, L is the cross-coupling coefficient , $Q(r_s)v_s$ is the flow rate of the water, σ is the electrical conductivity of the water, K is the hydraulic conductivity of the water and $|r - r_s|$ is the distance between the base electrode and the roving electrode. The flow rate of the water in the spring, the electrical conductivity and the distance between the base electrode and the roving electrode were directly measured, a typical cross-coupling coefficient was chosen from the Sheffer and Oldenburg paper, and the hydraulic conductivity was estimated through trial and error. To model the flow two point injection wells were constructed on either side of the peaks of the experimental data to estimate fluid flow coming up across that whole area.

An image reconstruction was done from Hammann et al., (1997) to construct images of what the subsurface looks like beneath each of the three lines. This is not specifically a modelling technique, but just a method to reconstruct an image of the subsurface to observe the positions of

the positive and negative SP sources. The image reconstruction is very useful for determining the depths of the sources which can not be obtained from collecting the data on the surface.

The Hammann method was adapted from an approach of Di Maio and Patella (1994) which involved a multiple source location method, which was based on an assumption that a system of a number of elementary or point sources can unambiguously represent SP signals. The spatial distribution of these elementary sources are established via the image reconstruction (Hammann et al., 1997).

The algorithm behind the image reconstruction technique involves determining the lateral and depth coordinates of SP sources, such that other geological, geophysical and hydrogeological information can be correlated precisely with the interpreted positions of the SP sources. This reduces the ambiguity involved in distinguishing between likely sources of SP anomalies from SP contour maps and profiles.

The basis behind the algorithm is that it is assumed that the potential differences ΔV measured between two electrodes with spacing Δx;

$$\frac{\Delta V}{\Delta X} \approx \frac{\partial V}{\partial x} = E_{x_{meas}}$$

Can be characterised explicitly as the superposition of horizontal components of electrical field produced by n elementary sources with arbitrary strength:

$$E_{x_{meas}} = \sum_{i=1}^{n} E_x^i$$

The problem reduces to attaining a collection of elementary sources that adequately explain the measured data ($E_{x_{meas}}$). The horizontal electrical field component of a unit line source is (e.g., Telford et al., 1990);

$$E_{x=}\frac{x}{x^2+z^2}$$

Where x represents the horizontal distance from the source and z represents the source depth. A grid search procedure was used to find electrical sources that could create the observed SP signals.

The first step involved defining a scanner function $g(x_j, a, b)$ to represent the horizontal electrical field component at the surface due to a point source located at position (a, b):

$$g(x_j, a, b) = \frac{(x_j - a)}{(x_j - a)^2 + (-b)^2}$$

The second step involved calculating the cross-correlation coefficient between $E_{x_{meas}}$ and $g(x_j, a, b)$ for each position $\hat{C}(a, b)$;

$$\hat{C}(a, b) = \sum_j g(x_j, a, b)\, E_{x_{meas}}(x_j)$$

and this equation was normalised to contrast cross-correlation coefficients associated with sources at different depths which led to values of C between ±1 which is represented as contours in the images (Figures 12,13,14):

$$C(a, b) = \frac{\hat{C}(a, b)}{[\sum_j g^2(x_j, a, b) \sum_j E^2_{x_{meas}}(x_j)]^{1/2}}$$

The third step involved using the maxima and minima of $C(a,b)$ to define the positions of the positive and negative point SP sources (Figures 12,13,14).

After obtaining the images of the subsurface an SP Modelling technique from Fathianpour (1997) was used to model the flow paths in the subsurface. The program is generally used for modelling SP effects from minerals but the same concepts apply in modelling with groundwater. The program was called SP2D and it implements a solution for the SP based on a macroscopic physical model proposed originally in a paper by Eskola and Hongisto (1987). The technique involves creating an input file that models what the subsurface flow looks like (Figures 18,19,20) then running the program and obtaining good output models (Figures 15,16,17) that correlate well with the SP signals. The inverting is done manually through trial and error until a good model is fitted to the data.

The self-potential associated with groundwater flow in an electrolytic environment is modelled by assuming a primary source as an electric double layer between the flowing groundwater and the porous media created by the flowing SP currents. This primary flow generates the secondary surface charge and double layers on the interfaces between media with different conductivities.

The theory behind this forward modelling technique is that a linear interpolation over triangular subdomain elements of the unknown SP effect is used, which is known as a 2-D finite element (FE) formulation. Then a system of linear equations is derived from a Galerkin weighting technique and these linear equations approximate the governing partial differential equations, then the linear system of equations is solved by a banded matrix equation solver (Fathianpour, 1997).

Discussion

The analytical method used to determine fluid flow from a point injection well produced a reasonable fit for all three lines with the fit with line C the best fitting model. In particular it was successful at fitting the heights and positions of the peaks of the SP responses but was not as successful for fitting the widths of the peaks due to the fact that the method involves a point source to the surface (Figures 9,10,11).

Figure 11 shows the correlation between the modelling and the moving average of the absolute voltages for line C. The peak for the unnamed spring at co-ordinates (680679, 6740616) (Figure 5) was the closest modelled out of the three peaks further enhancing the belief that the increase in the SP response here was solely from EK effects and not EC effects.

The correlation between the modelling and the moving average of the absolute voltage for line B is shown in Figure 10. For this line, the height of the Bubbler was very closely modelled but the width was very narrow, only approximately 100 m wide in the model compared to the 300 m width in the SP response. Again the unnamed spring at (680679, 6740616) was very closely modelled with the height and width at the top of the peak but the position was slightly off which could not be changed as this negatively affected the model.

For line A (Figure 9) the association between the modelling and the real data was not as close as the other two lines but this was expected to the rather less smooth nature of the profile. The positions of the two peaks were modelled closely but the heights and widths were not as so closely modelled. This may represent a greater influence of EC effect near the springs on this line than on the other lines. The large decrease in the self-potential response was also modelled to some extent.

The image reconstruction technique was very successful in getting a picture of the subsurface for the three lines (Figures 12,13,14). It gave a better understanding of where the SP sources came from and so provided a good estimate of where the water flow is occurring.

The image for line A (Figure 12) showed a positive elementary SP source for the 900 m peak at a depth of 5-150 m with the strongest part of the source coming from a depth of 30-100 m. The source to explain the peak at approximately 450 m did not show as well in the reconstruction but the source appears to be roughly 20-50 m deep. The source for the trough appears to be at a depth of 20-80 m but because there are no springs in this general area there is a high probability that this signal is generated from EC effects.

The image reconstruction done for line B (Figure 13) showed a complex network of SP sources and did not produce a high C value corresponding to any of the peaks for the line. The source underneath the Bubbler (Figure 5) was not defined very well in the image and the source could be from approximately 20-280 m deep. Interestingly a source of approximately at a depth of 20-250 m occurred below a peak not directly associated with a spring along the line although the line does go over the Little Bubbler runoff with the Little Bubbler roughly 70 m to the south-west of the line. This peak may be as a result of groundwater flow rising up towards the Little Bubbler. For the peaks associated with the other springs the depth of the sources are similar and are approximately 20-100 m deep.

A well defined SP source is seen at a depth of between 30-140 m underneath Blanche Cup (Figure 5) along Line C (Figure 14). The depth for the SP source for the spring 1000 m along the line is between 5-140 m. This image reconstruction shows a connection between the SP sources between the two springs which indicates a strong probability of an interconnection between the

SP sources for the two springs. As expected the image for the first 600 m contain a number of different shallow SP sources generated from EC effects.

The numerical modelling technique from Fathianpour (1997) produced nice fitting models (Figures 15,16,17) for all three lines and in the process developed groundwater flow networks for each line to see how the groundwater is flowing in the subsurface. For Line A the flow network (Figure 18) connects at roughly 50 m depth and for the Little Bubbler the width of the flow column is 200 m wide at 50 m depth which corresponds to the width of the peak from the SP response. This might suggest a fault at this depth. The width then gets thinner as you get closer to the surface to about 35m. The other spring contains a consistent width of 160 m from 50 m depth to approximately 25m.

For Line B the flow network (Figure 19) connected at a much deeper depth of 135 m compared to line A with the width of The Bubbler being the largest at 140m wide which roughly corresponded to the peak from the SP response. To obtain a nice fit for the model The Bubbler flow path was shifted to the south east for the top twenty or so metres. A flow path was constructed at approximately 1250 m which was 100 m wide to also help fit the model. This says that there is a flow path in one of the deep aquifers in this region which may represent a fault.

For Line C the flow network (Figure 20) also connected at a very deep depth of 330 m with the flow paths getting wider the closer towards the surface at approximately 160 m suggesting that the aquifers get larger or there are is a larger fault network in this area. Blanche Cup had a width of 180 m from 160 m upwards which corresponded nicely with the peak in the SP response.

Conclusion

This research provides new information about the flow of groundwater beneath the mound springs from the GAB to the LEB. It was seen that undertaking SP surveys near spring systems is a useful geophysical method to see groundwater flow and should be used more often in the future to gain an even better understanding of groundwater flow near the margins of the GAB. It was observed for all lines that the flow pipes are connected at various depths in the subsurface through an aquifer which could possibly be either the Algebuckina Sandstone or the Cadnaowie Formation.

Undertaking the SP survey in a very heterogeneous area was not ideal due to the EC effects associated with chemical reactions in the soils and the other geophysical techniques performed were not as successful as SP in detecting groundwater flow. It is still inconclusive to say exactly how the water flows up whether due to faults or seepage but the very wide flow paths for some springs suggest seepage to be more probable here.

Acknowledgements

First of all, the author would like to thank my supervisor Graham Heinson and co-supervisor Michael Hatch for their constant support, assistance and inputs throughout the entire year in helping getting this thesis done. I would also like to thank Kent Inverarity for his discussions and assistance with fieldwork and also for helping me with modelling and the image reconstructions.

I would also like to thank my fellow honours students of 2011, particularly the hydrogeophysics students, for the fun times we experienced throughout the year on field trips, field work and throughout every day in the office which greatly lowered my stress levels. Thanks to Kat and

Chris from Heading Bush Outback Adventures for providing such a wonderful home away from home during the two and a half weeks of fieldwork, which gave more time for actually doing fieldwork and daily data processing.

Also thanks my family for their constant support and understanding throughout the year, the National Water Commission for funding the Great Artesian project, the University of Adelaide for providing resources throughout the whole year and also additional funding from the Australian Society of Exploration Geophysicists Scholarship.

References

AIZAWA K., YOSHIMURA R., OSHIMAN N., YAMAZAKI K., UTO T., OGAWA Y., TANK S. B., KANDA W., SAKANAKA S., FURUKAWA Y., HASHIMOTO T., UYESHIMA M., OGAWA T., SHIOZAKI I. & HURST A. W. 2005. Hydrothermal system beneath Mt. Fuji Volcano inferred from magnetotellurics and electric self-potential. *Earth and Planetary Science Letters* **235**, 1-2.

BEDROSIAN P. A., UNSWORTH M. J. & JOHNSTON M. J. S. 2007. Hydrothermal circulation at Mount St. Helens determined by self-potential measurements. *Journal of Volcanology and Geothermal Research* **160**, 137-146.

CORRY C. E., DEMOULLY, G.T., GERETY, M.T. 1983. *Field Procedure Manual For Self-Potential Surveys*. Zonge Engineering & Research Organisation, Tucson, Arizona.

CORWIN R. F. 1990. The self-potential method for environmental and engineering applications, Volume 1: Review and Tutorial. *Society of Exploration Geophysicists, Tulsa, OK*.

DEPARTMENT OF ENVIRONMENT AND RESOURCE MANAGEMENT 2011. *The Great Artesian Basin*. **W68**.

DI MAIO R. & PATELLA D. 1994. Self-potential anomaly generation in volcanic areas; the Mt. Etna case-history. *Acta Vulcanologica* **4**, 119-124.

ESCOLA L. A. H., H. 1987. A Macroscopic Physical Model for the Self Potential of a Sulphide Deposit. *Geoexploration* **24**, 219-226.

FAGERLUND F. & HEINSON G. 2003. Detecting subsurface groundwater flow in fractured rock using self-potential (SP) methods. *Environmental Geology* **43**, 782-794.

FAN Y. & DENG S. 2002. Theoretical and experimental studies of membrane potential in shaly sands for improved Rw calculation. *Petrophysics Houston Tex* **43**, 119.

FATHIANPOUR N. 1997. A Finite Element Program for Modelling Mineral SP Effects of 2-D Earth Structures.

FRIENDS OF MOUND SPRINGS 2007. *President's Message*.

GEOLOGICAL SURVEY OF SOUTH AUSTRALIA 1992. *Curdimurka*.

HABERMEHL M. A. 1982. Springs in the Great Artesian Basin, Australia; their origin and nature. *Report Bureau of Mineral Resources Geology and Geophysics* **234**.

HABERMEHL M. A. 2001. Hydrogeology and environmental geology of the Great Artesian Basin, Australia. *Special Publication Geological Society of Australia* **21**, 127-143.

HABERMEHL R. 1996. Groundwater movement and hydrochemistry of the Great Artesian Basin, Australia. *Abstracts Geological Society of Australia* **43**, 228-236.

HAMMANN M., MAURER H. R., GREEN A. G. & HORSTMEYER H. 1997. Self-Potential Image Reconstruction: Capabilities and Limitations. *Journal of Environmental and Engineering Geophysics* **2**, 21-35.

ISHIDO T. & MIZUTANI H. 1981. Experimental and theoretical basis of electrokinetic phenomena in rock-water systems and its applications to geophysics. *Journal of Geophysical Research* **86**, 1763-1775.

JOUNIAUX L., MAINEULT A., NAUDET V., PESSEL M. & SAILHAC P. 2009. Review of self-potential methods in hydrogeophysics. *Comptes Rendus Geoscience* **341**, 10-11.

KIM S., HEINSON, H., JOSEPH, J. 2004. Electrokinetic Groundwater Exploration: A New Geophysical Technique. *CRC LEME, School of Earth and Environment Sciences*.

LYKLEMA J. 1995. Fundamentals of Interface and Colloid Science. **Volumes I,II,III**.

MUDD G. M. 2000. Mound Springs of the Great Artesian Basin in South Australia: a case study from Olympic Dam. *Environmental Geology* **39**, 463-476.

NATIONAL HERITAGE TRUST 2005. Hydrology of Lake Eyre Basin.

SCHIAVONE D. & QUARTO R. 1984. Self-potential prospecting in the study of water movements. *Geoexploration* **22**, 47-58.

SHEFFER M. R. & OLDENBURG D. W. 2007. Three-dimensional modelling of streaming potential. *Geophysical Journal International* **169**, 839-848.

SILL W. R. 1983. Self-potential modeling from primary flows. *Geophysics* **48**, 76-86.

TORGERSEN T., HABERMEHL M. A. & CLARKE W. B. 1992. Crustal helium fluxes and heat flow in the Great Artesian Basin, Australia. *Chemical Geology* **102**, 139-152.

Figure Captions

Figure 1: Map of the Great Artesian Basin (GAB)

Figure 2: Location of The Bubbler and Blanche Cup springs in the Wabma Kadarbu National Park and other Spring complexes in the area.

Figure 3: Generalised cross-section of the Great Artesian Basin showing aquifers, confining layers and direction of water flow.

Figure 4: Stern Model of the Electrical Double Layer with two different circumstances. For A, the zeta-potential is negative because there is not a large amount of specific adsorption between the pore wall and plane H, and for B, vice versa

Figure 5: Wabma Kadarbu Area showing the three SP lines, green dots representing springs and the locations of the Blanche Cup and the Bubbler spring.

Figure 6,7,8: These figures show profiles of the SP response across all three lines. They show both the absolute voltages, three-point moving average absolute voltages and they also show elevation.

Figure 9,10,11: These figures show the Analytical Modelling for all three lines. The heights of the peaks are modelled well but the widths are not as well modelled

Figure 12,13,14: These figures show the Image Reconstructions for all three lines showing the correlations of charge locations and SP observations.

Figure 15,16,17: These figures show the Numerical Modelling for all three lines. The models here fit better than for the Analytical Modelling.

Figure 18,19,20: These figures show the groundwater flow path networks for all three lines obtained from the numerical modelling. The depths of the flow paths and widths are labelled. All three networks have very similar geometries which are expected as they are in the same area.

Figures

Figure 1 (Mudd et al. 2000)

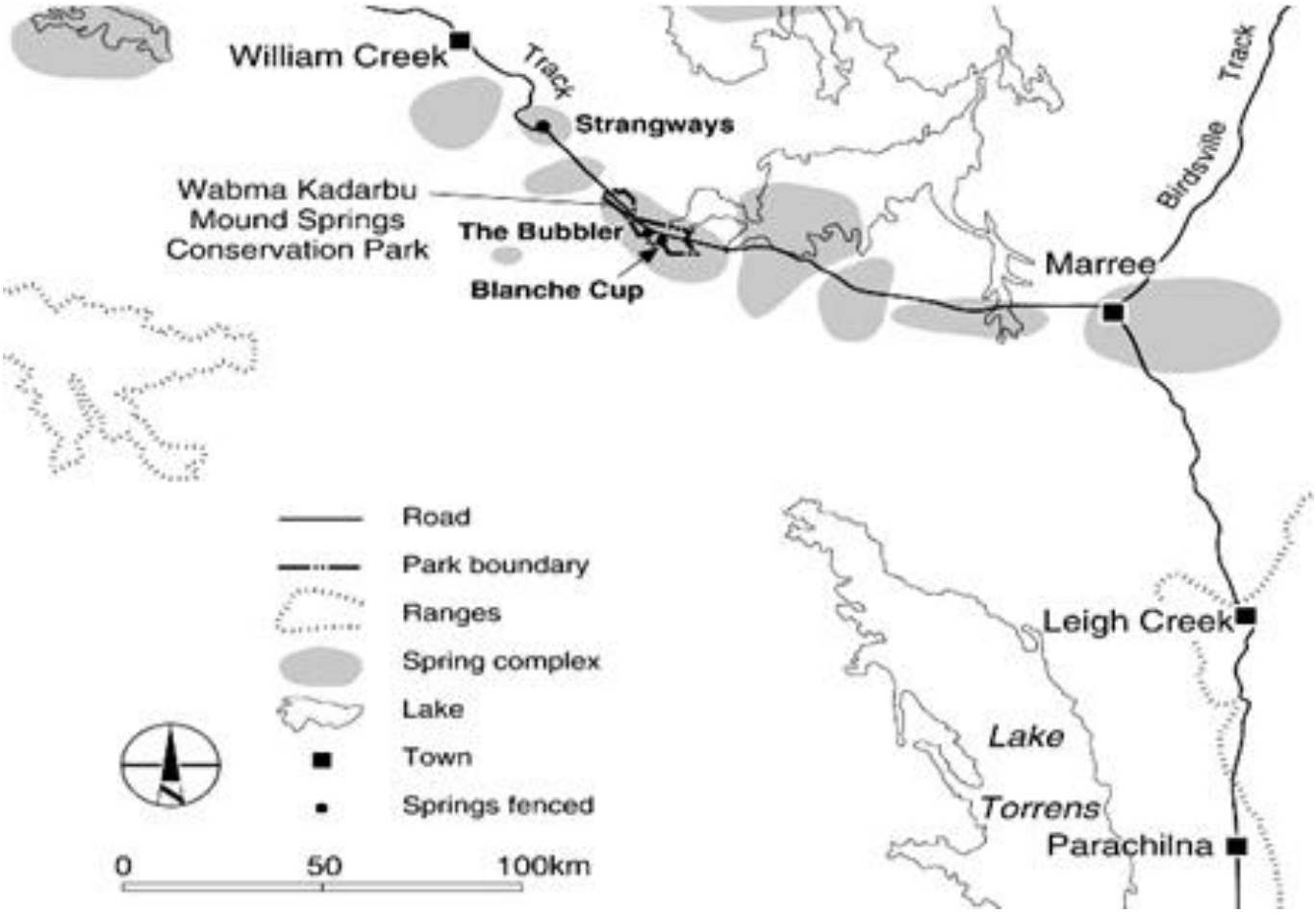

Figure 2 (Friends of Mound Springs,2007)

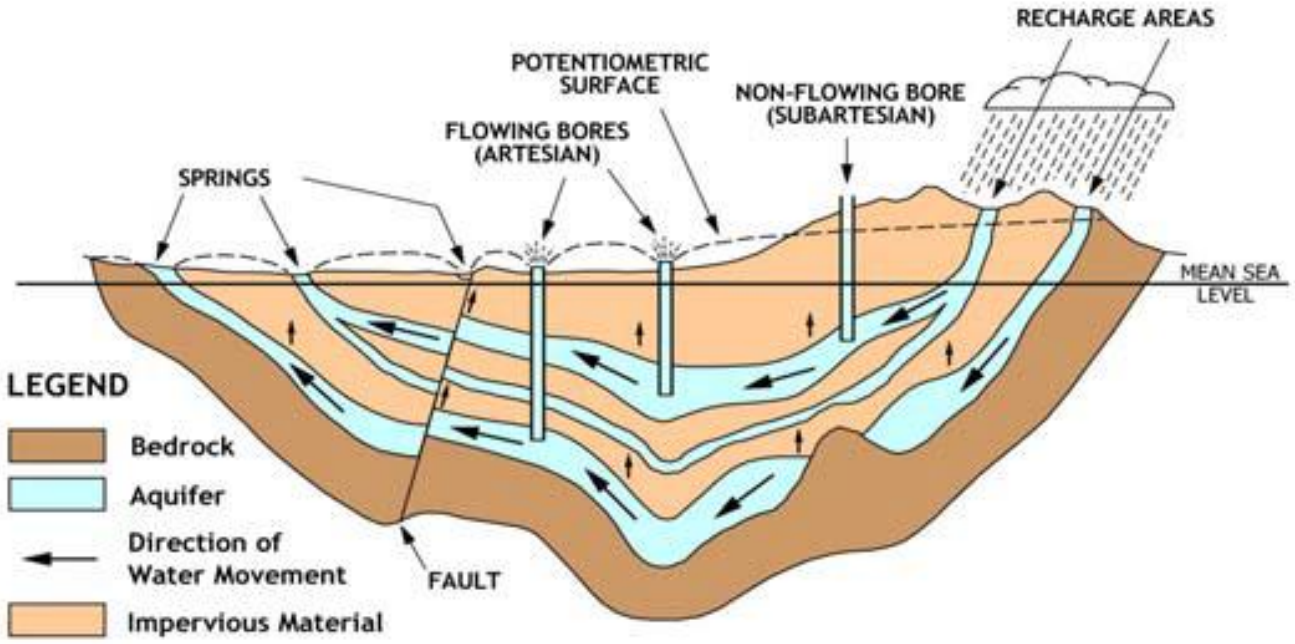

Figure 3 (Department of Environment and Resource Management, 2011)

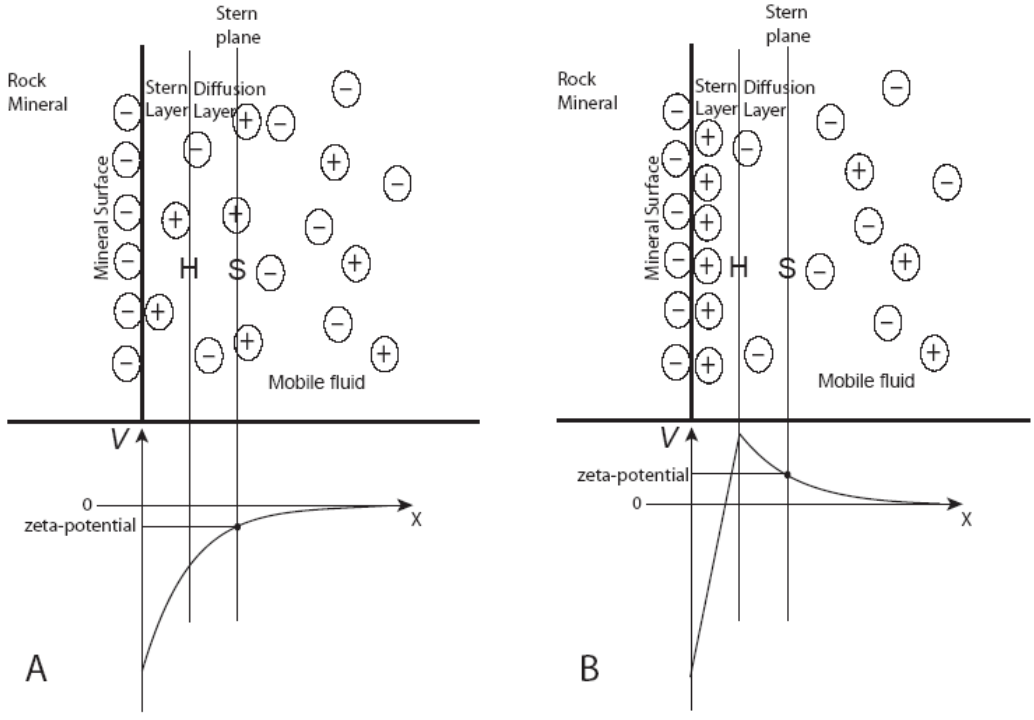

Figure 4 (Kim et al. 2004)

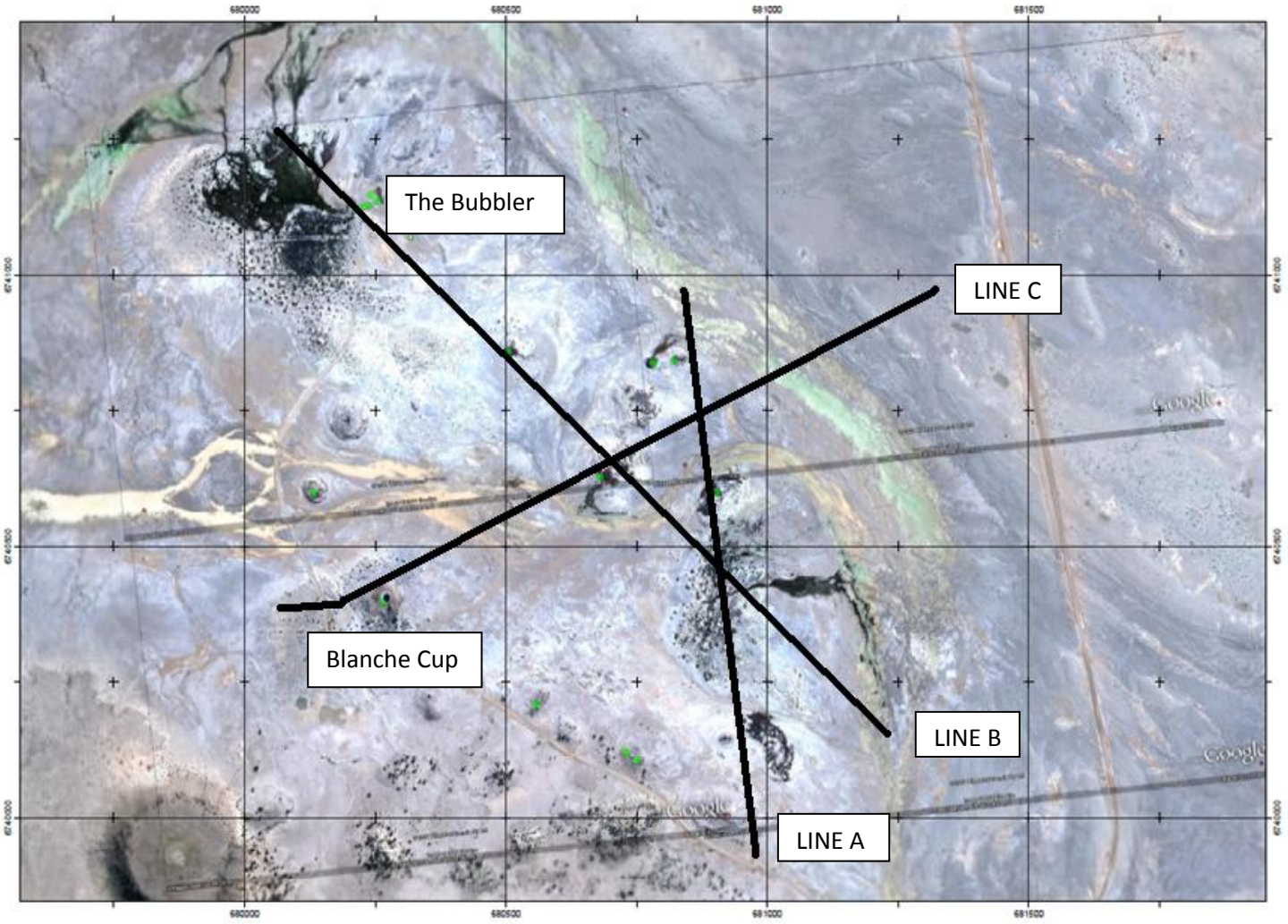

Figure 5 (Google Earth, 2011)

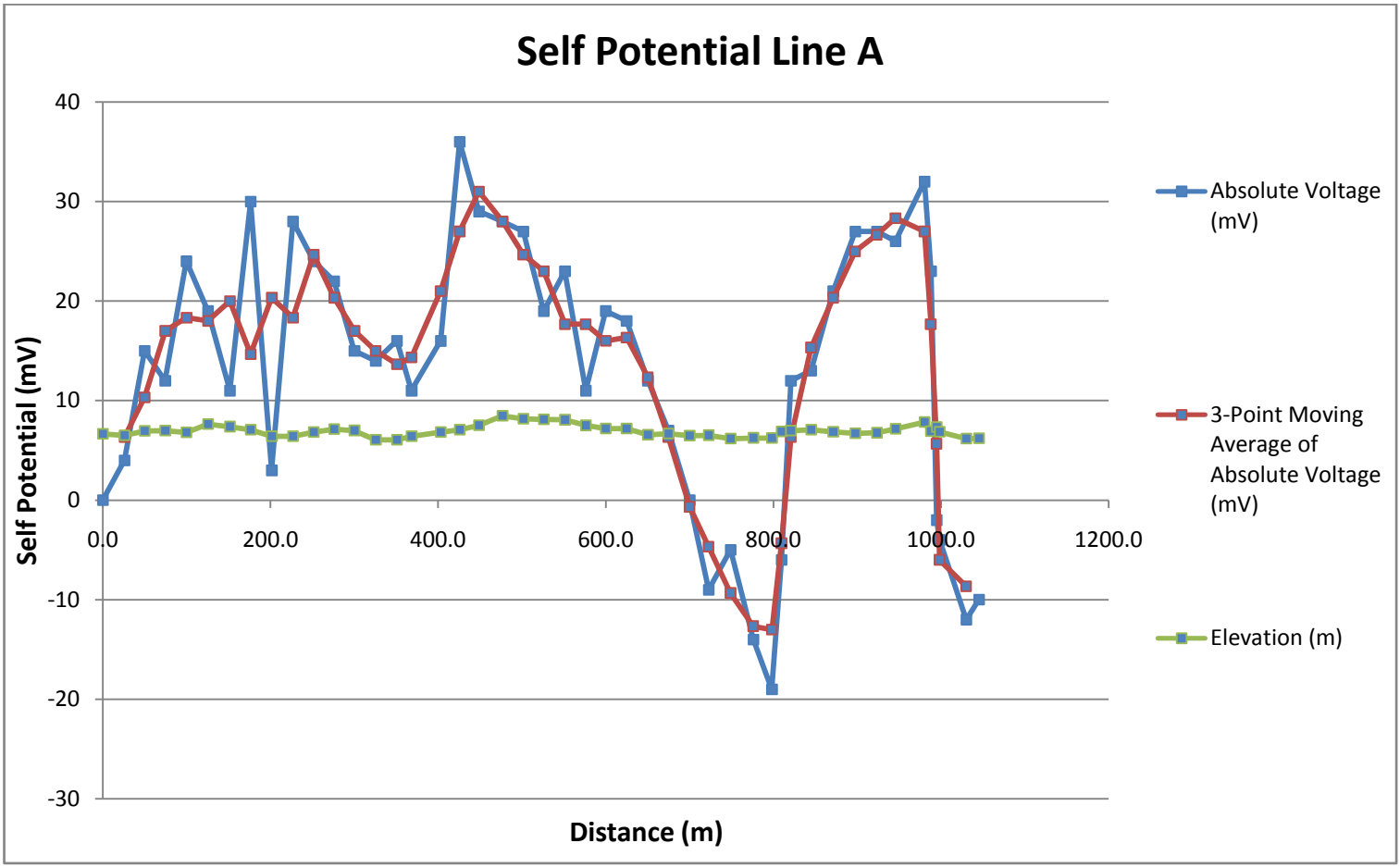
Self Potential Line A
40
30
20
10
0
-10
-20
-30
0.0
200.0
400.0
600.0
800.0
1000.0
1200.0
Self Potential (mV)
Distance (m)
Absolute Voltage (mV)
3-Point Moving Average of Absolute Voltage (mV)
Elevation (m)

Figure 6

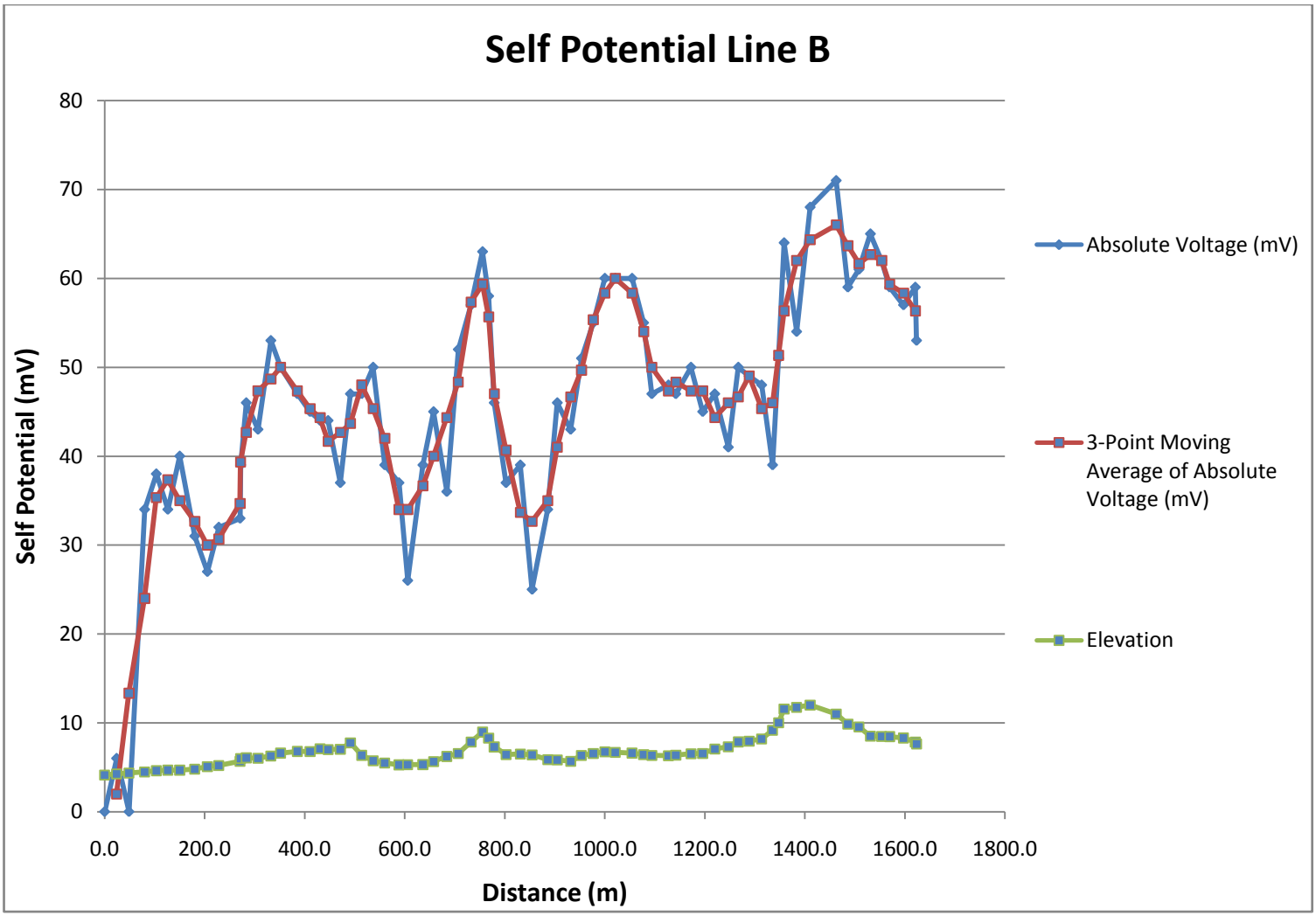
Self Potential Line B
Self Potential (mV)
80
70
60
50
40
30
20
10
0
0.0
200.0
400.0
600.0
800.0
1000.0
1200.0
1400.0
1600.0
1800.0
Distance (m)
Absolute Voltage (mV)
3-Point Moving Average of Absolute Voltage (mV)
Elevation

Figure 7

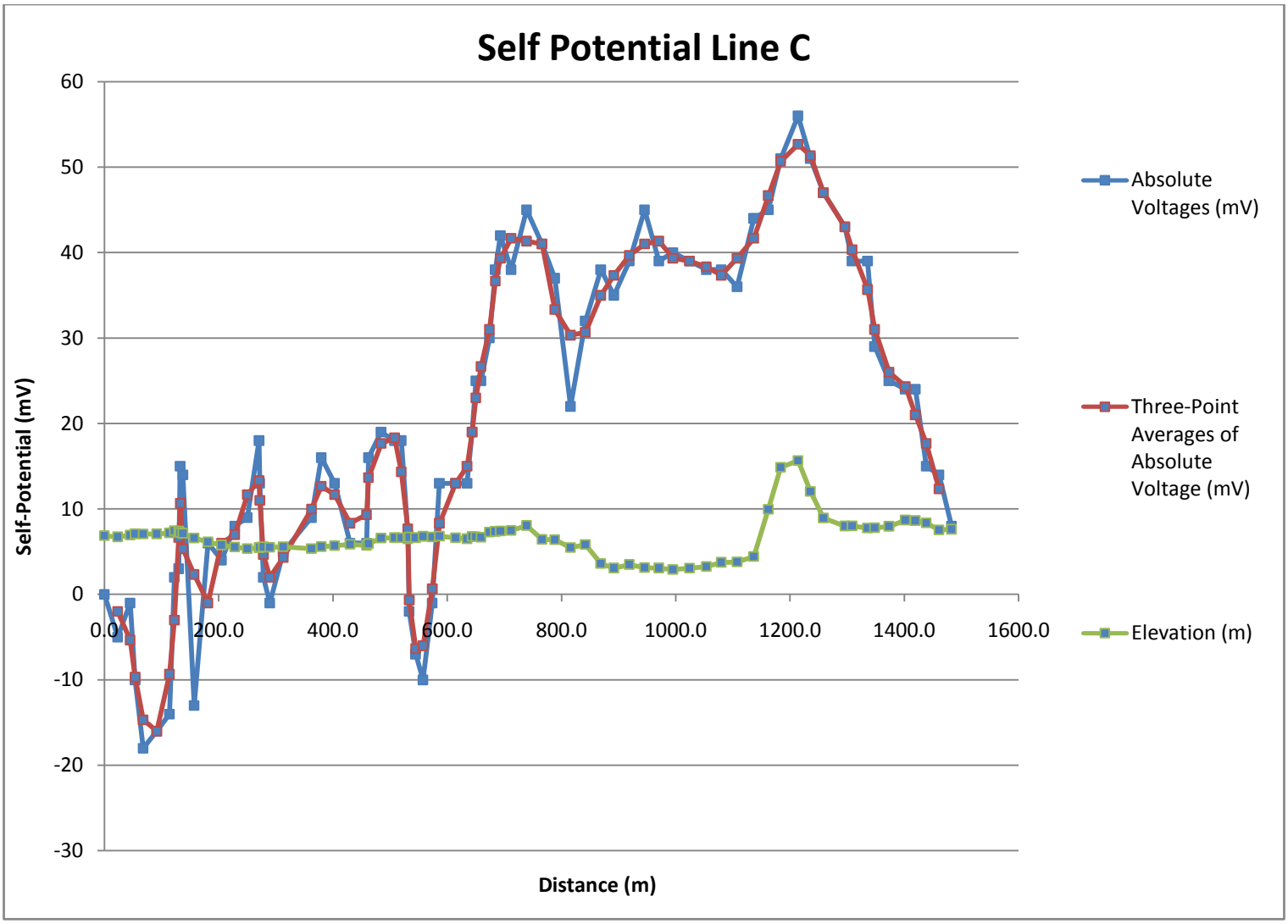
Self Potential Line C
60
50
40
30
20
10
0
-10
-20
-30
Self-Potential (mV)
0.0
200.0
400.0
600.0
800.0
1000.0
1200.0
1400.0
1600.0
Distance (m)
Absolute Voltages (mV)
Three-Point Averages of Absolute Voltage (mV)
Elevation (m)

Figure 8

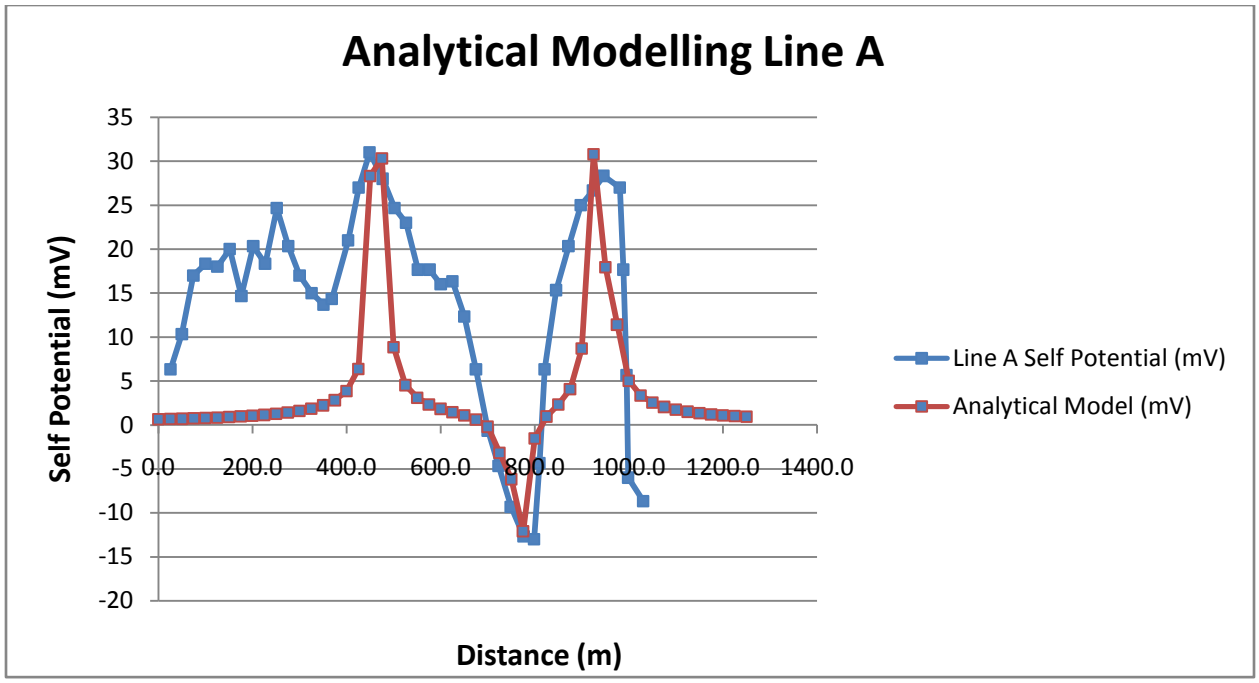
Analytical Modelling Line A
Self Potential (mV)
35
30
25
20
15
10
5
0
-5
-10
-15
-20
0.0
200.0
400.0
600.0
800.0
1000.0
1200.0
1400.0
Distance (m)
Line A Self Potential (mV)
Analytical Model (mV)

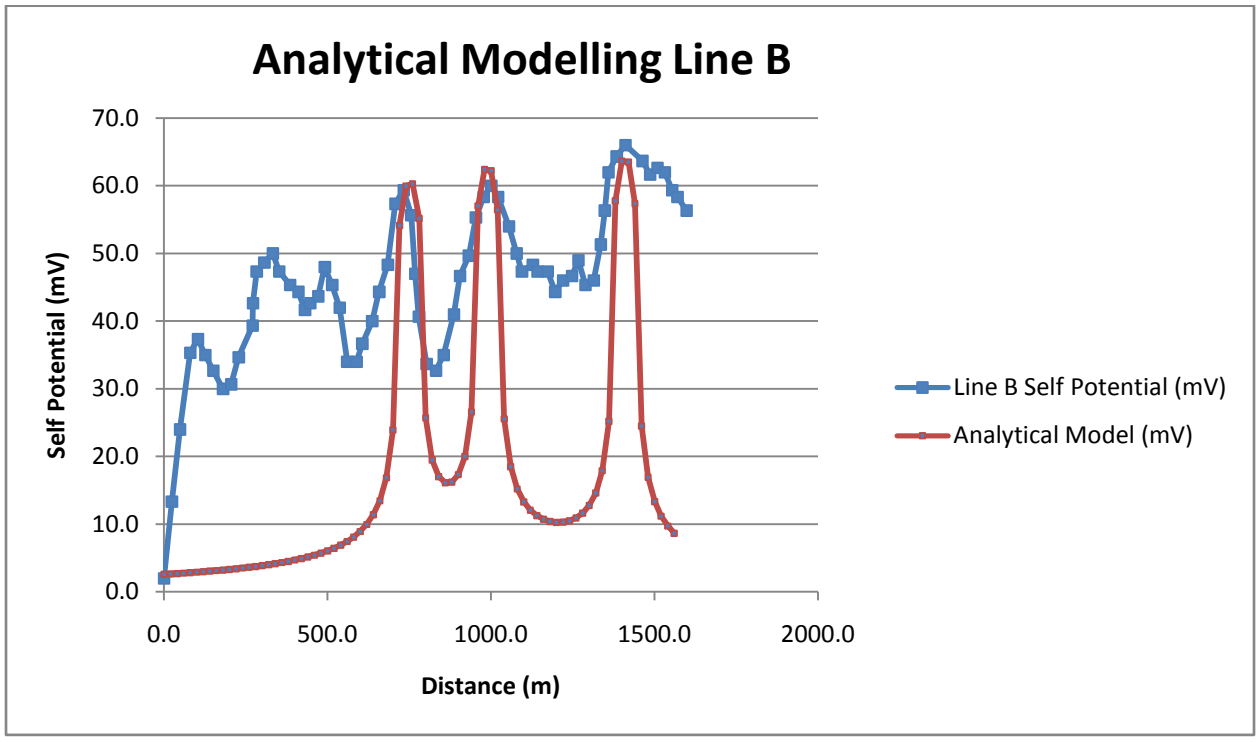
Analytical Modelling Line B
Self Potential (mV)
70.0
60.0
50.0
40.0
30.0
20.0
10.0
0.0
0.0
500.0
1000.0
1500.0
2000.0
Distance (m)
Line B Self Potential (mV)
Analytical Model (mV)

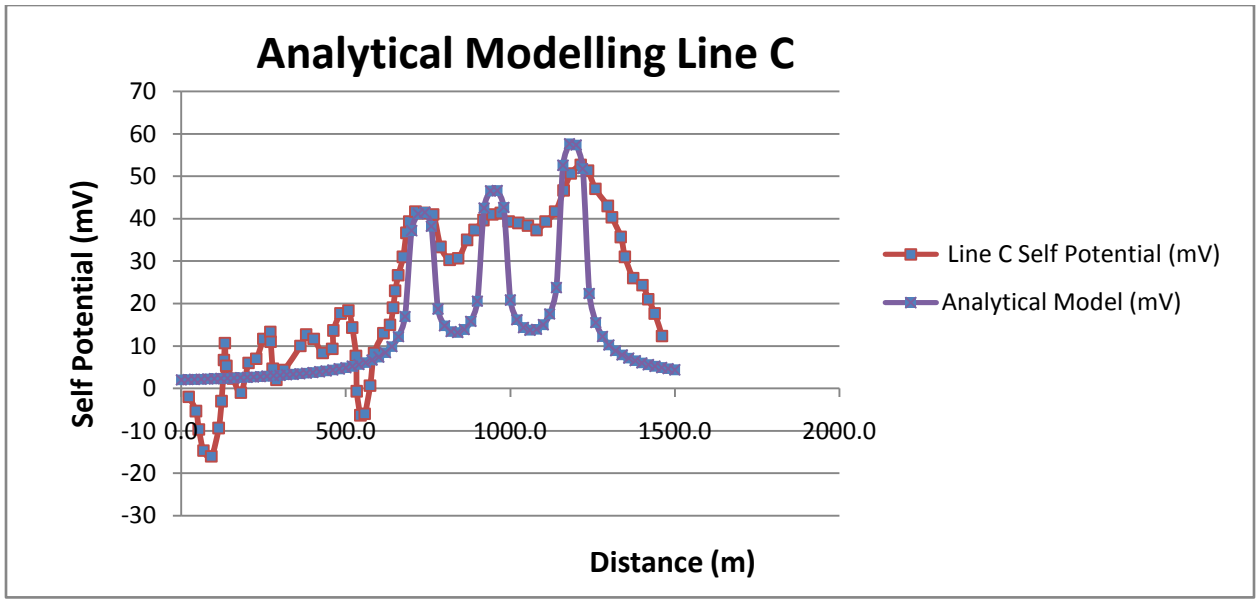

Figures 9,10,11

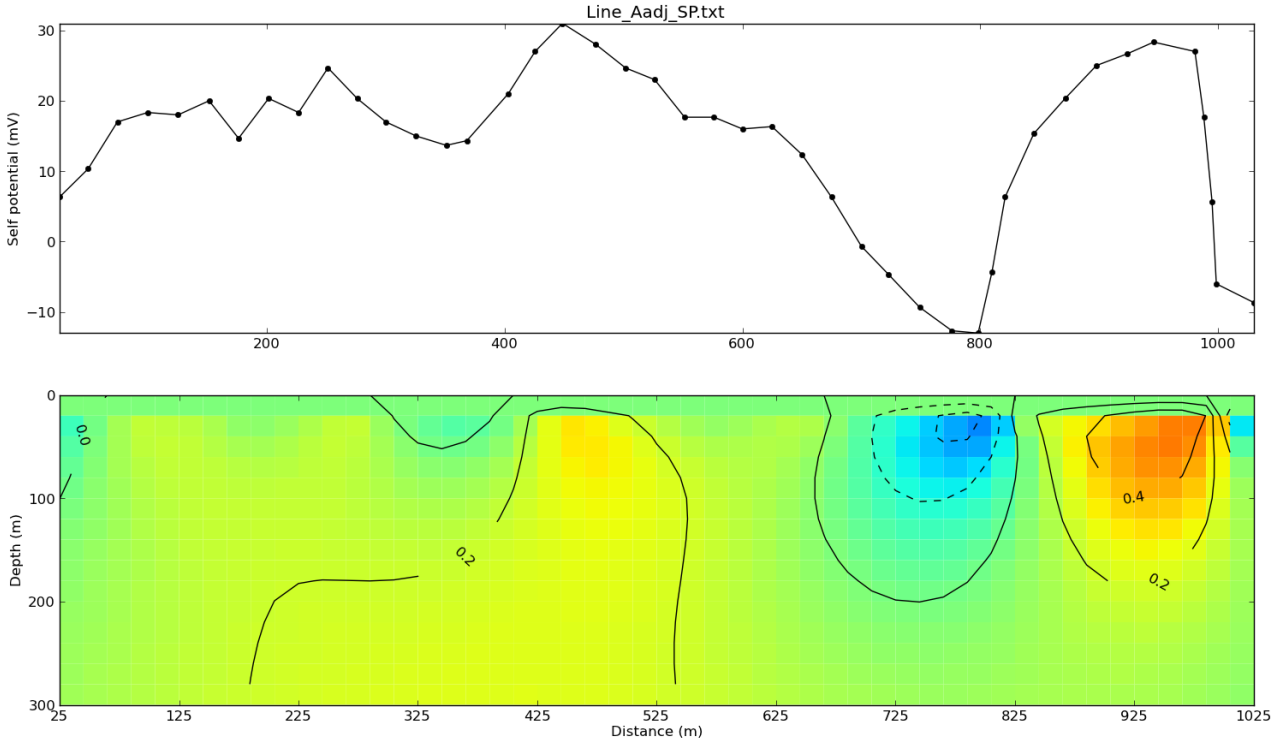

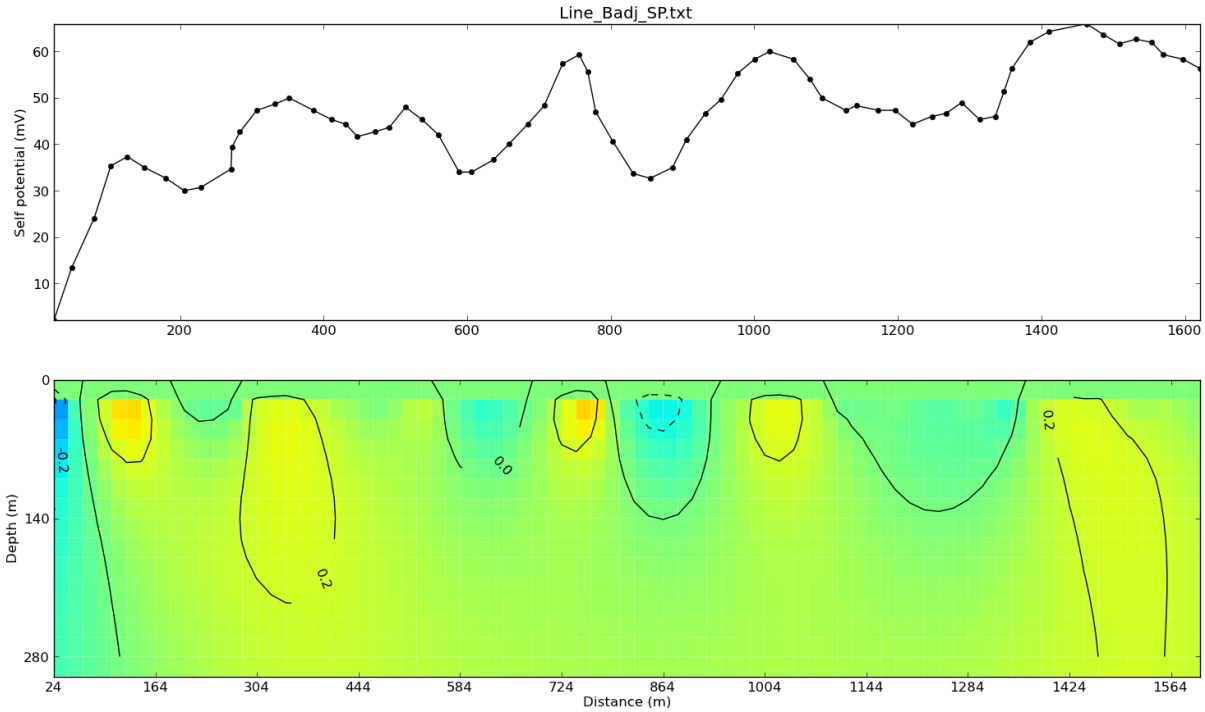

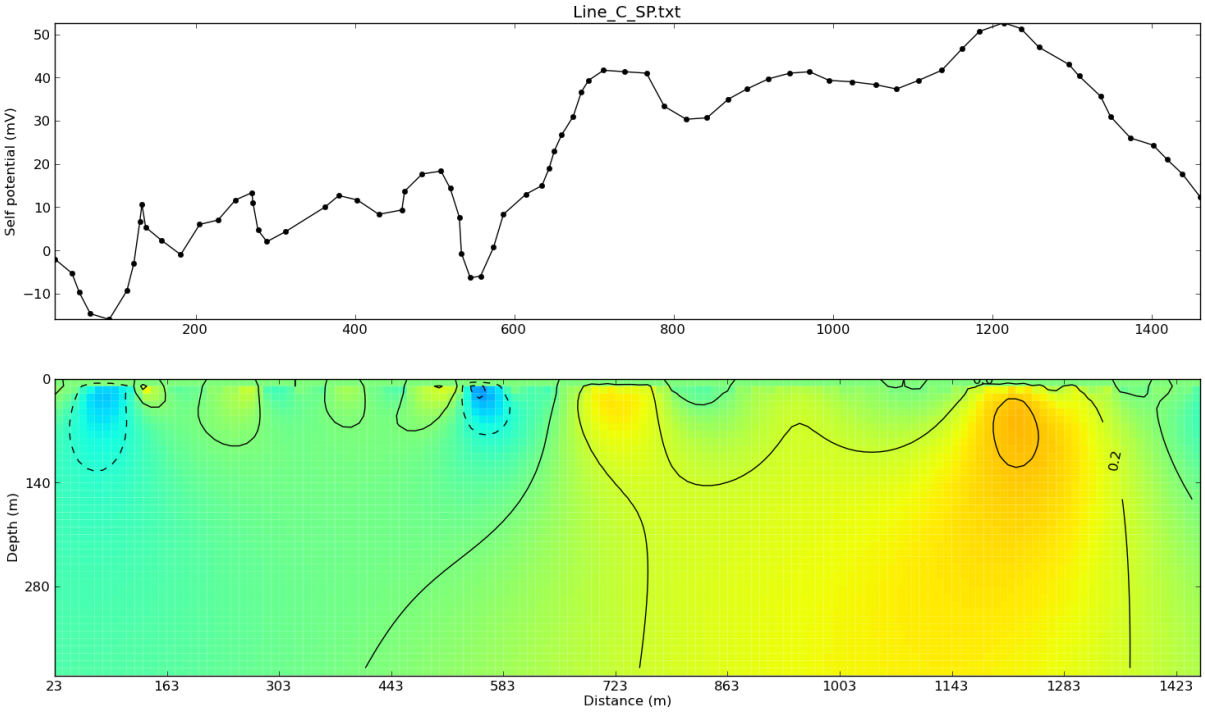

Figures 12,13,14

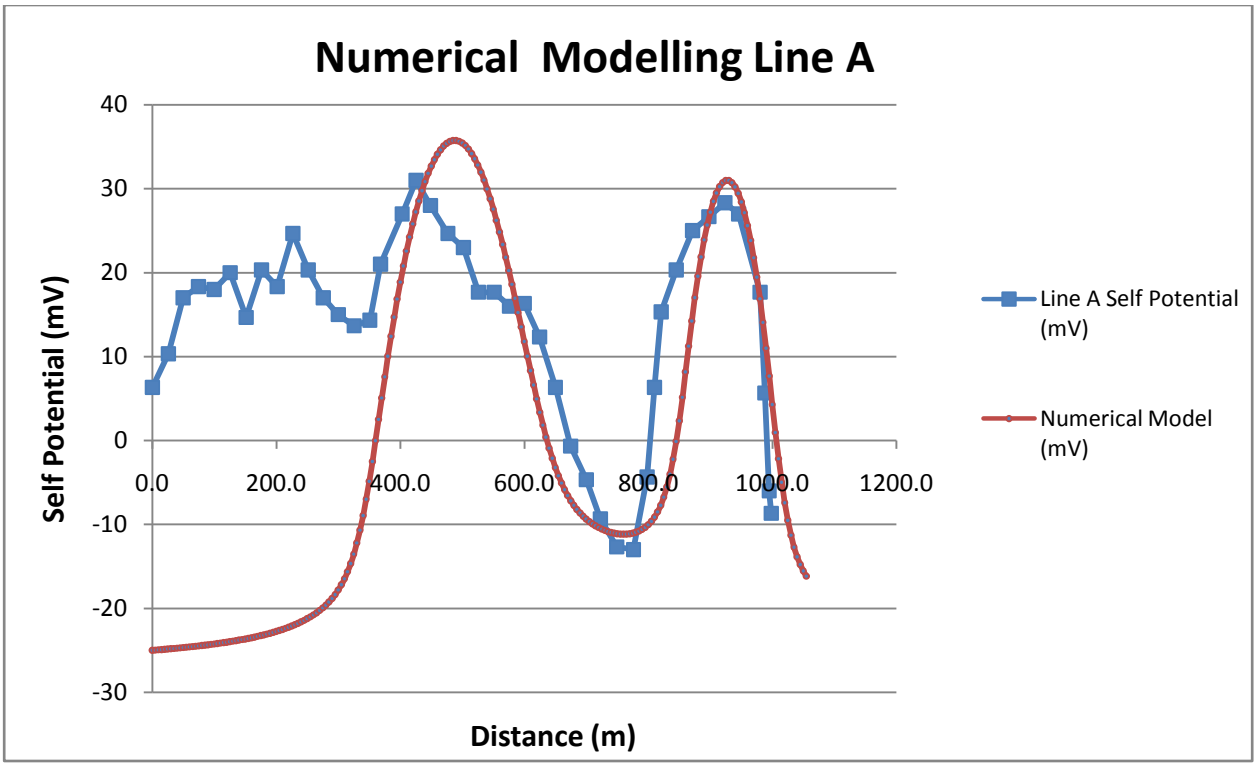
Numerical Modelling Line A
Self Potential (mV)
40
30
20
10
0
-10
-20
-30
0.0
200.0
400.0
600.0
800.0
1000.0
1200.0
Distance (m)
Line A Self Potential (mV)
Numerical Model (mV)

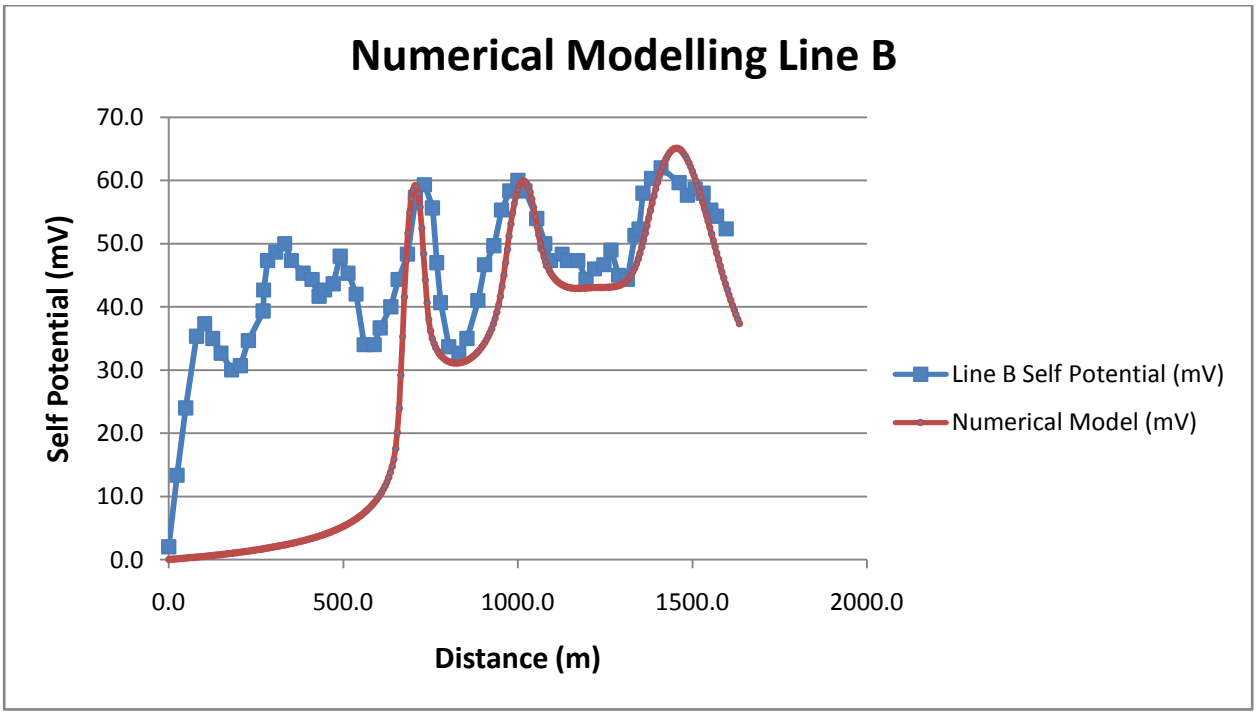
Numerical Modelling Line B
Self Potential (mV)
70.0
60.0
50.0
40.0
30.0
20.0
10.0
0.0
0.0
500.0
1000.0
1500.0
2000.0
Distance (m)
Line B Self Potential (mV)
Numerical Model (mV)

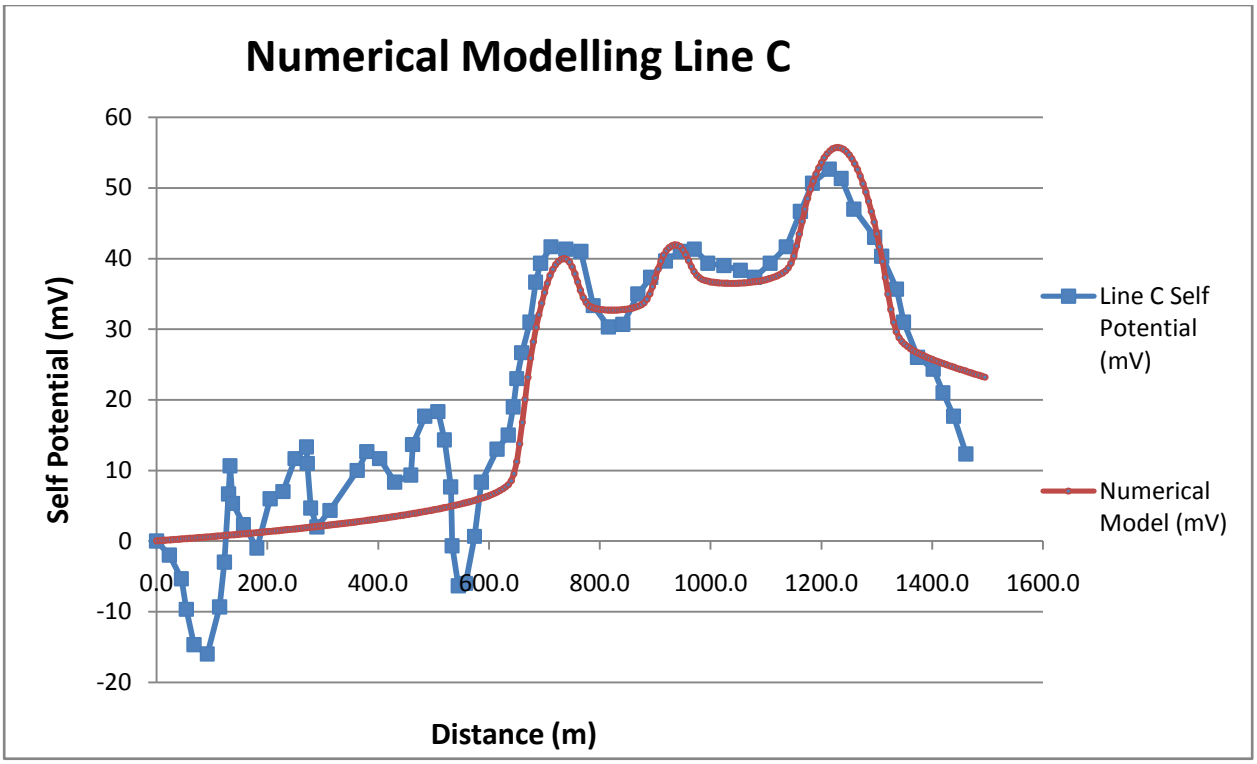

Figures 15,16,17

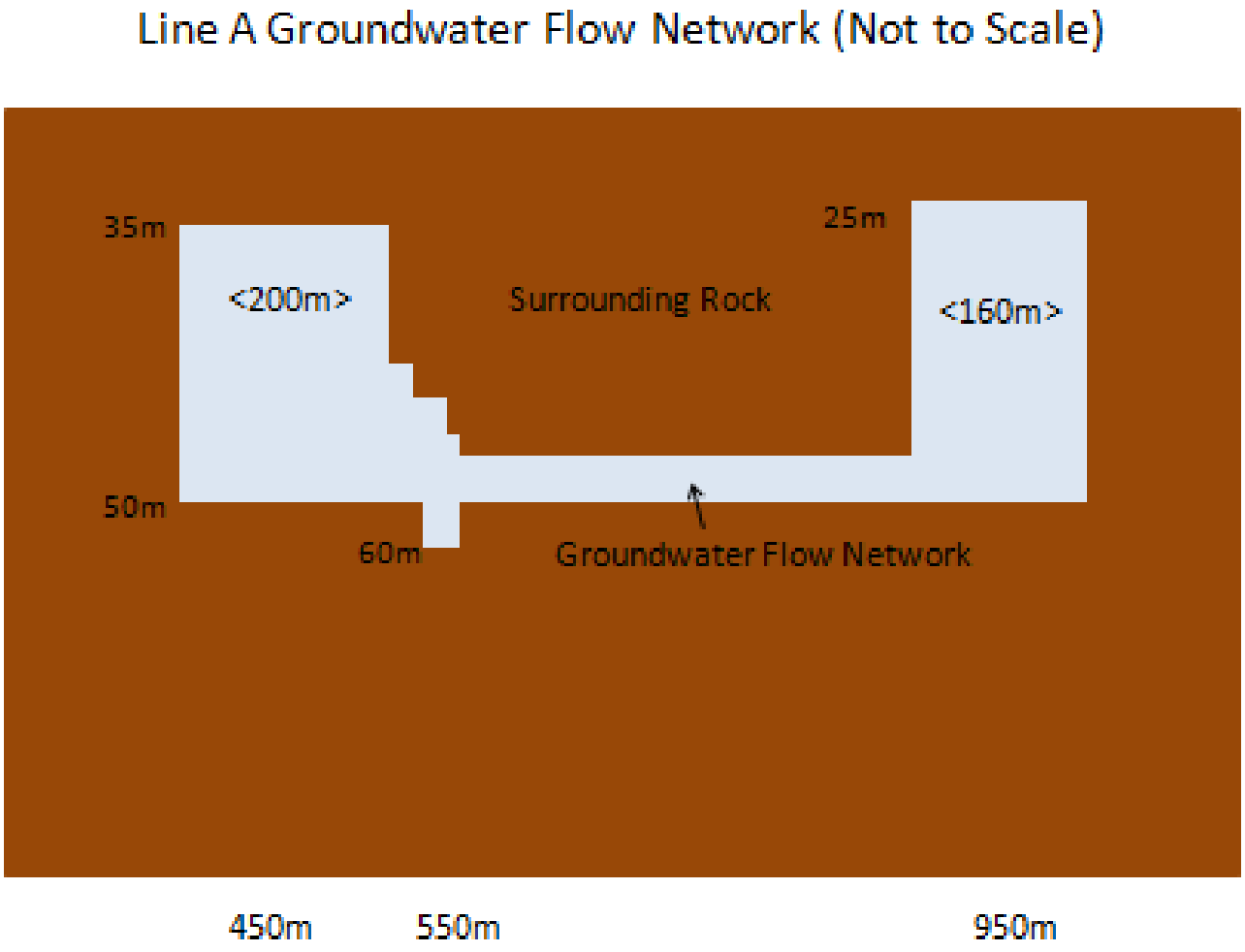
Line A Groundwater Flow Network (Not to Scale)
35m
25m
<200m>
Surrounding Rock
<160m>
50m
60m
Groundwater Flow Network
450m
550m
950m

Figure 18

Line B Groundwater Flow Network (Not to Scale)

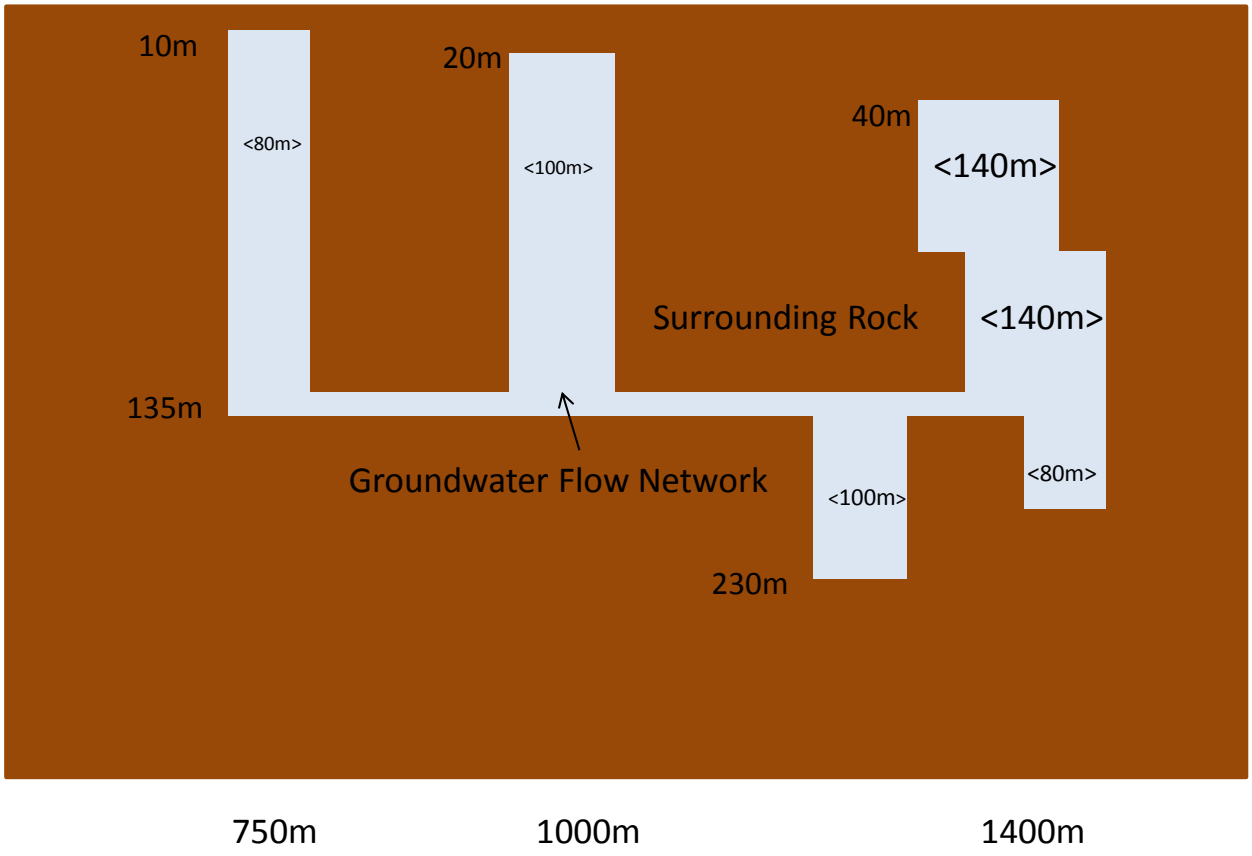

Figure 19

Line C Groundwater Flow Network (Not to Scale)

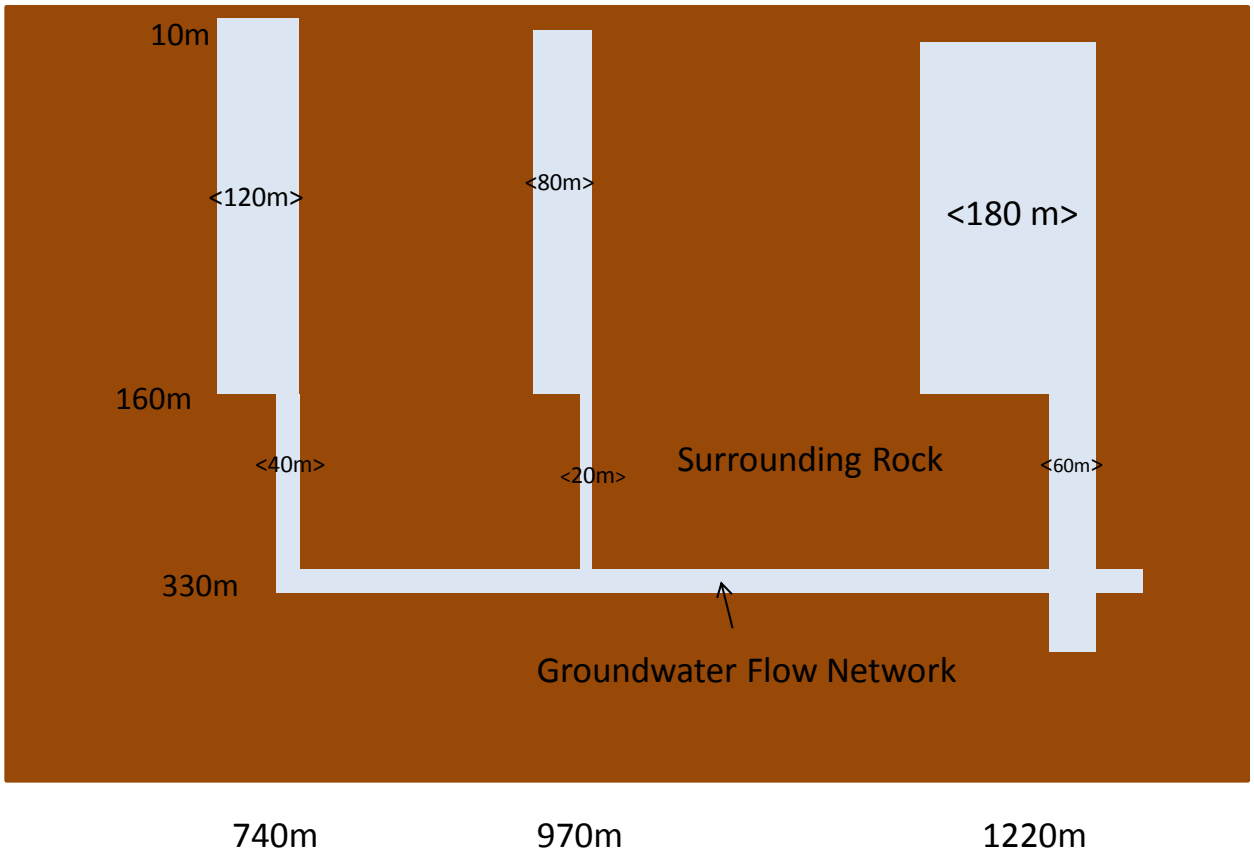

Figure 20

Appendices

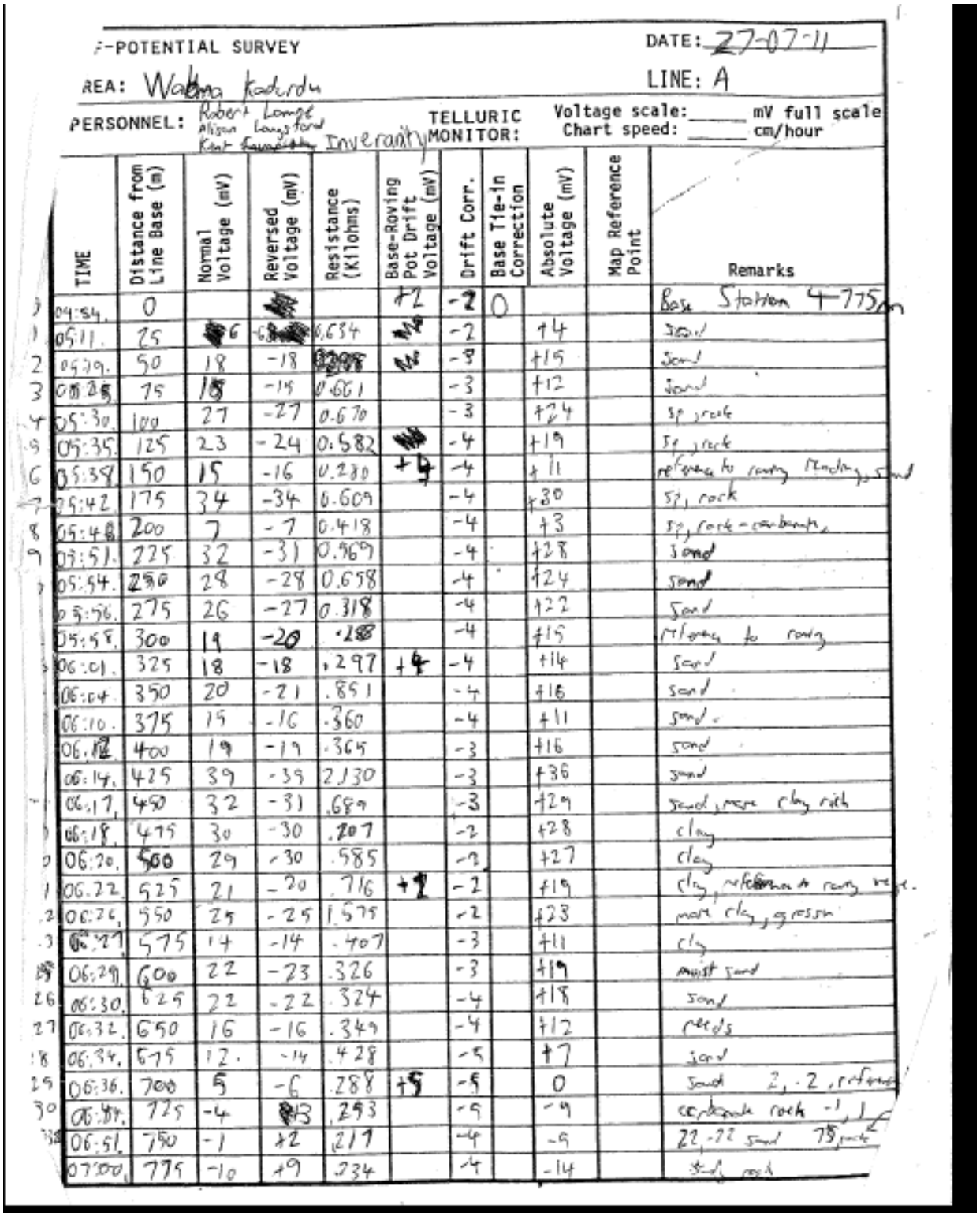

-POTENTIAL SURVEY

DATE: 27-07-11

AREA: Wakka Kadrdu

LINE: A

PERSONNEL: Robert Longe, Alison Longsford, Kent [illegible] Inveraray

TELLURIC MONITOR:

Voltage scale: _____ mV full scale

Chart speed: _____ cm/hour

	TIME	Distance from Line Base (m)	Normal Voltage (mV)	Reversed Voltage (mV)	Resistance (Kilohms)	Base-Roving Pot Drift Voltage (mV)	Drift Corr.	Base Tie-in Correction	Absolute Voltage (mV)	Map Reference Point	Remarks
	04:54.	0		[illegible]		+2	-2	0			Base Station 4-775m
1	05:11.	25	[illegible]6	-6 [illegible]	0.634	[illegible]	-2		+4		Sand
2	05:29.	50	18	-18	[illegible]	[illegible]	-3		+15		Sand
3	05:25.	75	18	-15	0.661		-3		+12		Sand
4	05:30.	100	27	-27	0.670		-3		+24		Sp, rock
5	05:35.	125	23	-24	0.582	[illegible]	-4		+19		Sp, rock
6	05:39.	150	15	-16	0.280	+4	-4		+11		reference to roving Readings, Sand
7	05:42.	175	34	-34	0.609		-4		+30		Sp, rock
8	05:48.	200	7	-7	0.418		-4		+3		Sp, rock = carbonate
9	05:51.	225	32	-31	0.969		-4		+28		Sand
	05:54.	250	28	-28	0.658		-4		+24		Sand
	05:56.	275	26	-27	0.318		-4		+22		Sand
	05:58.	300	19	-20	.288		-4		+15		reference to roving
	06:01.	325	18	-18	.297	+4	-4		+14		Sand
	06:04.	350	20	-21	.851		-4		+16		Sand
	06:10.	375	15	-16	.360		-4		+11		Sand.
	06:12.	400	19	-19	.365		-3		+16		Sand
	06:14.	425	39	-39	2.130		-3		+36		Sand
	06:17.	450	32	-31	.689		-3		+29		Sand, more clay rich
	06:18.	475	30	-30	.207		-2		+28		clay
0	06:20.	500	29	-30	.585		-2		+27		clay
1	06:22.	525	21	-20	.716	+1	-2		+19		clay, reference to roving [illegible].
2	06:24.	550	25	-25	1.575		-2		+23		more clay, gypsum
3	06:27.	575	14	-14	.407		-3		+11		clay
25	06:29.	600	22	-23	.326		-3		+19		moist sand
26	06:30.	625	22	-22	.324		-4		+18		Sand
27	06:32.	650	16	-16	.349		-4		+12		reeds
28	06:34.	675	12.	-14	.428		-5		+7		sand
29	06:36.	700	5	-6	.288	+5	-5		0		Sand 2, -2, reference
30	06:47.	725	-4	[illegible]3	.293		-5		-9		carbonate rock -1, 1
	06:51.	750	-1	+2	.217		-4		-5		22, -22 sand 75, rock
	07:00.	775	-10	+9	.234		-4		-14		Sand, rock

.LF-POTENTIAL SURVEY DATE: 27-07-11

AREA: Wabna Kadaba LINE: A

PERSONNEL: Robert Lange, Alina Langsford TELLURIC MONITOR: Voltage scale: ____ mV full scale; Chart speed: ____ cm/hour

	TIME	Distance from Line Base (m)	Normal Voltage (mV)	Reversed Voltage (mV)	Resistance (Kilohms)	Base-Roving Pot Drift Voltage (mV)	Drift Corr.	Base Tie-In Correction	Absolute Voltage (mV)	Map Reference Point	Remarks
034	07:04	800	-16	+15	.300		-3	0	-19		clay with log, pole, wire
035	07:08	825	+15	-15	.386		-3		+12		clay, wire, log
036	07:09	812.5	-4	+3	.260		-3		-16		" " + more wire
037	07:14	850	+15	-19	.305	+2	-2		+13		clay, less log, wire
		New Base 3	1st Jul 2011								
137	1:07	775	-4	+5	0.321	-1	+1	0	-8	N	Sandy rock from
138	1:08	800	-7	+7	0.379		+1		-6	N	Sandy gravel, fea
139	1:09	837	+24	-24	0.996		+1		+25	N	Sandy, gravel, fea
140	1:11	812.5	+9	-9	0.383		+1		+10	N	Sand, Gravel, Fea
141	1:15	850	+22	-21	0.956		+1		+23	N	Sandy, vegetation
142	1:18	875	+31	-30	0.649		+1		+32		Sandy ground
143	1:21	900	+37	-39	0.692		+1		+38		Sandy
144	1:24	925	+37	-37	1.470		+1		+38		Sandy, vegetation
145	1:27	950	+35	-34	1.070		+2		+37		Sandy, vegetation
146	1:31	975	+41	-41	0.773		+2		+43		Sandy, sand, gravel, rock
147	1:36	1000	+9	-6	0.329		+2		+34		Sandy, sand, gravel, rock
148	1:39	987.5	+7	-7	0.310		+2		+9		Sand, gravel, rock, Fern, Sand
149	1:42	975	+32	-33	0.853		+2		+7		Sandy, sand, gravel, rock
150	1:46	1000	-3	+3	0.293		+2		-1		Sandy, Sand, rock
151	1:49	1000	-1	+1	0.249	-2	+2		+1		Sandy, sand
		ground dries to 985m									
152	1:59	25	+19	-20	0.542	-3	+3		+31		Sand
153	2:02	50	+12	-14	0.352		+3		+22		certain rock
154	2:04	37.5	+12	-13	0.348		+3		+19		Sand
155	2:08	12.5	+28	-29	0.624	-3	+3		+15		Sand

SELF-POTENTIAL SURVEY

DATE: 28-07-11

AREA: Waba Kadorba

LINE: B

PERSONNEL: Robin Lange, Alison Bagford, Kari Lucenty

TELLURIC MONITOR:

Voltage scale: _____ mV full scale

Chart speed: _____ cm/hour

	TIME	Distance from Line Base (m)	Normal Voltage (mV)	Reversed Voltage (mV)	Resistance (Kilohms)	Base-Roving Pot Drift Voltage (mV)	Drift Corr.	Base Tie-in Correction	Absolute Voltage (mV)	Map Reference Point	Remarks
001	00:48					-3	+3	0			Bm 4775 M
002	01:07	0	-3	+3	.335		+3		0		Silty Sand
003	01:14	25	+3	-4	.371		+3		+6		mst silty sand mm clay
004	01:19	50	-3	+2	.312		+3		0		Sand, log
005	01:29	75	30	-30	.613		+4		+34		wet sand and clay mm
006	01:36	100	34	-33	.637		+4		+38		mst clayey sand
007	1:57	125	30	-30	.685		+4		+34		sand, rock <5cm deep
008	2:00	180	86	-37	.670	-4	+4		+40		sand, rock <5cm deep.
009	2:07	175	27	-25	.699		+4		+31		sand " " "
010	2:10	200	23	-24	.562		+4		+27		" " " "
011	2:22	229	28	-28	.563		+4		+32		clay sand
012	2:26	250	29	-29	.605		+4		+33		clay sand
13	2:30	275	42	-43	.733		+4		+46		Clay Sand, salt
14	2:34	262	+36	-35	.665		+4		+39		very clayey sand, salt
15	2:56	300	39	-38	.160	-4	+4		+43		very clayey sand, salt
16	2:59	325	49	-47	.852		+4		+53		clay, salt, mm silty sand
17	3:05	350	46	-47	.817		+4		+50		dry, sand, silt
18	3:08	375	43	-44	.787		+4		+47		dry, silt
19	3:18	400	41	-42	.760		+4		+45		dry, sand
20	3:33	925	39	-37	.680		+5		+44		moist clayey sand
21	3:38	450	39	-38	.695		+5		+44		moist clayey sand
22	3:44	475	32	-32	1.495		+5		+37		Sand, pebbles
23	3:44	500	42	-43	1.770		+5		+47		Sand "
24	4:08	525	42	-43	0.724		+5		+47		Sand "
25	4:13	550	45	-43	0.465	-5	+8		+50		Sand "
26	4:16	575	34	-35	0.629		+5		+39		Sand "
27	4:18	600	32	-37	0.595		+5		+37		Sand "
28	4:22	625	23	-18	0.389		+4		+26		Sand
29	4:24	650	35	-37	0.880		+4		+39		Sand, pebbles & rocks
30	4:26	675	41	-41	0.670		+4		+45		Sand with log
31	4:29	700	33	-33	0.616		+3		+36		clayey sand with log
32	4:31	725	49	-50	0.824		+3		+52		Sand

SELF-POTENTIAL SURVEY

DATE: 28-07-11

AREA: Wabna Kadarb

LINE: B

PERSONNEL: Robert Lange, Alison Longsford

TELLURIC MONITOR:

Voltage scale: _____ mV full scale

Chart speed: _____ cm/hour

	TIME	Distance from Line Base (m)	Normal Voltage (mV)	Reversed Voltage (mV)	Resistance (Kilohms)	Base-Roving Pot Drift Voltage (mV)	Drift Corr.	Base Tie-In Correction	Absolute Voltage (mV)	Map Reference Point	Remarks
33	4:33	750	54	-53	0.857	-3	+3		+57		
34	4:37	775	60	-61	0.937		+3		+63		Sand, over stony
35	4:39	800	43	-43	0.730		+3		+46		Sand
36	4:41	787.5	55	-55	0.981		+3		+58		Sand
37	4:43	825	35	-35	0.632		+2		+37		Sand
38	4:48	850	37	-37	0.643		+2		+39		gravel
39	4:51	875	23	-23	0.340		+2		+25		gravel - middle flat
40	4:53	900	32	-32	0.509		+2		+34		gravel
41	4:58	925	45	-44	0.767		+1		+46		more sandy gravel
42	5:01	950	42	-42	0.743		+1		+43		sandy gravel
43	5:03	975	50	-50	0.880		+1		+51		hill, on flat
44	5:05	1000	54	-54	0.310	-1	+1		+56		hill, sand
45	5:09	1025	59	-60	0.992		+1		+60		flat, on hill, gravel
46	5:11	1050	59	-55	0.940		+1		+60		hill, slope
47	5:13	1075	59	-60	0.991		+1		+60		flat, stony, on hill, ?
48	5:16	1100	54	-54	0.886		+1		+55		flat, sandy, gravel
49	5:18	1125	47	-47	0.810		0		+47		Flat, sandy, from hill
50	5:22	1150	48	-48	0.807		0		+48		Flat
51	5:26	1175	47	-47	0.804		0		+47		sandy, flat
52	5:28	1200	50	-50	0.846		0		+50		Sandy, flat, stony, rocky
53	5:31	1225	45	-46	0.799		0		+45		flat, sandy, loose stones, hill
54	5:34	1250	47	-47	0.783		0		+47		[illegible] sand, rocky, hill, stony
55	5:36	1275	+42	-43	0.744		-1		+41		sandy, flat
56	5:41	1300	+51	-50	0.850		-1		+50		Sandy, flat, pebbles, stones
57	5:47	1325	50	-50	0.524		-1		+49		rocky, on flat, near stones
58	5:49	1350	49	-48	0.830		-1		+48		Sandy, slope
59	5:57	1375	40	-41	0.787	+1	-1		+39		Sand, slope
											Base 1375m
156	4:00		54	56	317	+1	-1	+41			Sandy
155	4:04	25	+9	-9	0.298		-1		+48		Sandy
154	4:08	50	+13	-12	.302		-1		+53		Sandy
153	4:11	75	+9	-9	.334		-1		+49		Sandy

SELF-POTENTIAL SURVEY DATE: 28-07-11

AREA: Trafalgar Kadavu LINE: B

PERSONNEL: Robert Lange, Alison Langsford TELLURIC MONITOR: Voltage scale: _____ mV full scale; Chart speed: _____ cm/hour

	TIME	Distance from Line Base (m)	Normal Voltage (mV)	Reversed Voltage (mV)	Resistance (Kilohms)	Base-Roving Pot Drift Voltage (mV)	Drift Corr.	Base Tie-In Correction	Absolute Voltage (mV)	Map Reference Point	Remarks
160	4:13	100	-2	+1	0.483		-1		+38		Sandy
161	4:15	125	+19	-20	1.121		0		+60		Slope, sandy, pebbles
162	4:17	+125	+6	-7	0.389		0		+47		Sandy, slope, pebbles
163	4:20	150	+9	-10	0.347		0		+50		Sandy, flat
164	4:23	175	+22	-22	0.589		+1		+64		Sandy, black soil
165	4:28	250	+25	-24	0.379		+1		+67		Sandy, gravel
166	4:31	275	+13	-14	0.393		+1		+55		Sandy
167	4:34	300	+19	-16	0.319		+1		+57		wet, gravelly
168	4:36	325	+18	-19	0.339		+2		+61		wet, gravel
169	4:39	350	+15	-17	0.311		+2		+58		wet, gravel, pebbles, rocks
170	4:42	375	+12	-11	0.315		+2		+55		wet, muddy
171	4:46	400	+9	-11	0.387		+3		+53		wet, muddy, gravelly
172	4:49	425	+11	-9	0.311		+3		+56		wet, muddy, gravelly
173	4:51	430	+5	-7	0.310		+3		+49		dry, sandy
174	5:09	-25	16	-5	0.318	-3	+3		+50		Sandy
175	5:13	-50	+5	-5	0.341		+3		+49		Sandy
176	5:16	-75	+9	-10	0.310		+3		+53		Sandy
177	5:24	-125	+15	-15	0.386		+3		+59		Sandy
178		250	to 1050m								Sandy, Gravel
178	5:27	+125	+12	-11	0.314		+2		+55		Sandy, thick grass
179	5:29	+25	+15	-15	0.325		+2		+58		Low sand, grass
180	5:31	+325	+18	-18	0.322		+2		+61		Low sand, rocky, grass
181	5:34	+50	+8	-9	0.254		+2		+51		Rocky, gravel, more sandy
182	5:36	+0375	+15	-14	0.312		+1		+57		" "
183	5:38	-125	+24	-24	0.348		+1		+66		Sandy, rocky top, [illegible]
184	5:40	-6.25	+29	-28	0.569	-1	+1		+70		Sandy, Soil, dry stony [illegible]

SELF-POTENTIAL SURVEY DATE: 19-07-11

AREA: Waban Kaderbu LINE: C

PERSONNEL: Robert Longe, Alison Longford TELLURIC MONITOR: Voltage scale: _____ mV full scale; Chart speed: _____ cm/hour

TIME	Distance from Line Base (m)	Normal Voltage (mV)	Reversed Voltage (mV)	Resistance (Kilohms)	Base-Roving Pot Drift Voltage (mV)	Drift Corr.	Base Tie-In Correction	Absolute Voltage (mV)	Map Reference Point	Remarks
C1 00:00	0				-1	1	0			Base north-east granite [illegible]
C2 00:16	25	-6	+5	0.687		1		-5		pebbly sand
C3 00:24	50	-2	+2	0.816		1		-1		pebbly sand
C4 00:32	75	-19	+19	0.634		1		-18		gravel, sand
C5 00:25	625	-11	+12	0.606		1		-10		sand, pebbles
C6 00:28	100	-17	+17	0.510		1		-16		sand
C7 00:32	125	-15	+15	0.636		1		-14		Sand
C8 00:36	150	+14	-14	2.308		0		+14		Loose sand, sand dune
C9 00:38	137.5	+2	-2	0.797		0		+2		sand dune, rocky, boulders on plain
C10 00:41	145.75	+3	-4	1.760		0		+3		rocky, sand dune
C11 00:48	146.875	+19	-16	2.495		0		+15		loose sand, sand dune
C12 00:49	175	-13	+12	0.594		0		-13		pebbly Sand, [illegible]
C13 00:52	200	+6	-7	1.460	0	0		+6		pebbly sand
C14 00:57	225	+4	-4	0.598		0		+4		pebbly sand
C15 01:00	250	+8	-8	0.950		0		+8		Rock, lots Sponge
C16 01:02	275	+9	-10	0.702		0		+9		rocky Sand
C17 [illegible]	300	+18	-17	0.780		0		+18		rocky Sand
[illegible]	325	+1	+1	0.879		0		-1		wet pebbly sand after rain, Sponge
C19 1:12	312.5	+2	-3	0.604		0		+2		carbonate rocks, Sponge
C20 1:15	300.75	+13	-13	0.727		0		+13		Sand, wet
C21 1:21	350	+5	-6	0.512		0		+5		Schooled sand, rocks
C22 1:38	400	+9	-10	0.687	6	0		+9		river Creek, rocks, Sponge, over rocks
C23 1:43	425	+16	-17	0.758		0		+16		Sand, compact, rocky, Sponge
C24 1:46	450	+13	-14	1.154		0		+13		carbonate rock
C25 1:48	475	+6	-7	0.647		0		+6		compact rocky Sand
C26 1:52	500	+6	-4	0.680		0		+6		rocky, Sponge
C27 1:55	525	+19	-20	0.760		0		+19		Salt, rocks, river from [illegible]
C28 1:57	512.5	+16	-17	0.712		0		+16		Salt, rocks, river from [illegible]
C29 2:00	550	+18	+19	0.753		0		+18		Silty, rocky, flat, river [illegible]
C30 2:04	575	-2	+2	0.559		0		-2		Silty, rocky, flat.
C31 2:07	562.5	+18	-19	0.760		0		+18		rocky ground
C32 2:09	568.75	+7	-8	0.614		0		+7		Silty Sand

SELF-POTENTIAL SURVEY

DATE: 29-07-11

AREA: Wobma Kokorbo

LINE: C

PERSONNEL: Rosie Lowe, Allan Langford

TELLURIC MONITOR:

Voltage scale:______ mV full scale

Chart speed:______ cm/hour

	TIME	Distance from Line Base (m)	Normal Voltage (mV)	Reversed Voltage (mV)	Resistance (Kilohms)	Base-Roving Pot Drift Voltage (mV)	Drift Corr.	Base Tie-in Correction	Absolute Voltage (mV)	Map Reference Point	Remarks
93	2:12	600 m	-10	+11	0.567	0	0		-10		flat rocky
94	2:19	682.5	-7	+6	0.517		0		-7		"
95	2:22	625 m	+13	-11	0.622		0		+13		"
96	2:34	612.5	-1	+1	0.509		0		-1		"
97	2:40	650 m	+13	-13	0.650		0		+13		"
98	2:45	675 m	+13	-12	0.616		0		+13		Flat rocky
99	2:47	700 m	+25	-26	0.877		0		+25		Flat, silty bog, near spring
100	2:49	687.5	+28	-25	0.758		0		+25		Flat, silty
101	2:51	681.25	+19	-19	0.654		0		+19		Flat, silty
102	2:55	725 m	+42	-43	0.971		0		+42		sandy, flat
103	2:58	712.5	+30	-31	1.015		0		+30		Slope, near spring, sandy
104	3:00	718.75	+38	-37	0.594		0		+38		sandy, moist
105	3:04	750 m	+38	-38	1.220		0		+38		sandy, mostly vegetation, near rock spring
106	3:10	775 m	+45	-46	0.925		0		+45		mostly sandy
107	3:15	800 m	+41	-42	0.938		0		+41		wet, highly covered vegetation
108	3:18	825	+37	-36	0.861		0		+37		muddy, wet sand
109	3:32	850	+22	-23	0.678		0		+22		Sandy, plain flat, rocky
110	3:56	875 m	+32	-32	0.785		0		+32		Silty, lower flat
111	3:58	900 m	+38	-37	0.857		0		+38		Sandy, moist, flat
112	4:01	925 m	+35	-36	0.836		0		+35		Sandy, wet, flat
113	4:04	950 m	+39	-39	0.831		0		+39		Carbonate rock, vegetation
114	4:13	975 m	+45	-45	0.912		0		+45		Compact, clay, sandy, moist
115	4:18	1000 m	+39	-39	0.838	[illegible] 0	0		+39		sandy, silty, vegetation
116	4:21	1025 m	+40	-40	0.853		0		+40		Sandy, silty
7	4:23	1050 m	+39	-39	0.844		0		+39		Sandy, silt, clayey bits
8	4:26	1075 m	+38	-37	0.849		0		+38		Sandy, silt, clayey bits
9	4:29	1100 m	+38	-39	0.838	[illegible]	0		+38		sandy, less clay
6	4:31	1125 m	+36	-36	0.890		0		+36		sandy, clay bits
1	4:33	1150	+44	-43	0.560		0		+44		Clay, silty, bits, slope
	4:41	1175	+45	-45	0.951		0		+45		rock, slope
	4:54	1200	+50	-51	1.029		0		+51		rock, slope, before Black C
	4:59	1225	+56	-57	1.420	[illegible]	0		+56		rock, slope, after Black C

SELF-POTENTIAL SURVEY

DATE: 29-07-11

AREA: Wolima Kadisha

LINE: E

PERSONNEL: [illegible]
Alison Langsford

TELLURIC MONITOR: Voltage scale: ____ mV full scale
Chart speed: ____ cm/hour

	TIME	Distance from Line Base (m)	Normal Voltage (mV)	Reversed Voltage (mV)	Resistance (Kilohms)	Base-Roving Pot Drift Voltage (mV)	Drift Corr.	Base Tie-in Correction	Absolute Voltage (mV)	Map Reference Point	Remarks
125	6:03	1250	+51	-51	1.302		0		+51		Sandy, dark [illegible]
126	5:07	1275	+46	-46	0.450		1		+47		Sandy, dark [illegible]
127	6:05	1300	+42	-42	0.874	[illegible]	1		+43		Sandy, [illegible]
128	6:07	1325	+38	-38	[illegible]		1		+39		Sandy, [illegible]
129	6:10	1350	+38	-38	6.67	[illegible]	1		+39		Sandy, [illegible]
130	6:13	1375	+28	-27	2.435		1		+29		Sandy, pebbles, grey
131	6:20	1400	+24	-25	1.146		1		+25		Sandy, pebbles, [illegible]
132	6:22	1425	+22	-22	0.679		2		+24		[illegible] Sand, [illegible]
133	6:25	1450	+22	-23	0.624	[illegible]	2		+24		Sand, [illegible]
134	6:27	1475	+18	-13	0.552		2		+15		[illegible] clay, [illegible]
135	6:29	1500	+12	-13	0.439		2		+14		[illegible] clay, [illegible]
136	6:33	1525	+6	-5	0.432		2		+8		gravel, sand, clay, flat
						-2					gravel, [illegible] clay, flat